METHOD FOR THE DETERMINATION OF THE NOISE FROM TURBOJET AIRCRAFT ON TAKE-OFF TRAJECTORIES

Michel Kobrynski

NASA TTF-10,351

N67 10225

FACILITY FORM 602

(ACCESSION NUMBER)

(THRU)

(PAGES)

(CODE)

(NASA CR OR TMX OR AD NUMBER)

(CATEGORY)

02

GPO PRICE $ _____

CFSTI PRICE(S) $ _____

Hard copy (HC) _____ 2.50 _____

Microfiche (MF) _____ .75 _____

ff 653 July 65

TABLE OF CONTENTS

C_a Speed of sound in ambiant air

D Diameter of the outlet tube

f_{es} Frequency emitted by stationary jets

f_{ev} Frequency emitted by the jet in flight

f_a Apparent frequency, $f_a = \dfrac{1}{(1 + M \cos\theta_M)} f_{ev}$

f_c Central frequency of a band or an octave, $f_c = \sqrt{f_c \ f_{c+1}}$

Δf_c Magnitude of the filter band $\Delta f_c = f_{c+1} - f_c$ (octave: $\Delta f_c = f_c$)

I Acoustic intensity (power of flux) $I \cdot \dfrac{\overline{p^2}}{\rho C_a}$

I_0 Reference intensity $I_0 = 10^{-12}$ w/m^2

I_m Average acoustic intensity at the distance r from an isotropic source

$$I_m \cdot W_s / 2\pi r^2 \text{ on the ground}$$

I·D· Directivity index ID = 10 log Q (θ)

I·D_c Directivity index relative to the total level

I·D_i Directivity index relative to the octave i

K Nondimensional coefficient in the expression for W_s

ℓ Distance from a line parallel to the axis of the jet

M Mach number of the aircraft, $M = V_e/C_a$

M_c Mach number of convection of the turbulence $M_c = \tfrac{1}{2}\dfrac{V_j}{C_a}$ /6

M_j Jet Mach number $M_j = \dfrac{V_j}{C_a}$

n Number of turbojets of the aircraft (3.1.1.3.)

K_i Ordinate of the generalized spectrum of the acoustic pressure and the acoustic power

$N(\theta)$ Total acoustic pressure level, at the distance r, in the direction θ

$N_i(\theta)$ Acoustic pressure level of the octave i, at the distance r in the direction θ

N_m Total average acoustic pressure level at the distance r from an isotropic source

$$N_m = 20 \log \frac{r_m}{r}$$

iv

N_{mi} Average acoustic pressure level of the octave i

N_s Maximum total acoustic pressure level of the stationary jet

N_{si} Maximum total acoustic pressure level of the stationary jet of the octave i

N_f Spectral level of the acoustic pressure

N_w Total acoustic pressure level $N_w = 10 \log \frac{W_i}{W_o}$

N_{wi} Acoustic pressure level of the octave i

N_T Total acoustic pressure level of an aircraft with several jets

P Acoustic pressure

P_0 Reference pressure $P_o = 20 \mu R$

P_m Average total spatial pressure

P_{mi} Average spatial pressure of octave i

P Instantaneous pressure   <u>/7</u>

P_0 Average static pressure (the effective acoustic pressure is

$$P \cdot \sqrt{\overline{(P \cdot P_o)^2}}$$

$Q(\theta)$ Directivity factor, $Q(\theta) = P^2(\theta)/P_m^2$

r Distance from the source to the observation point

r_0 Reference distance

S Outlet surface of the tube

S_0 Reference surface

t Time

T_{ij} Characteristic tensor of a quadruplet

V Characteristic velocity

V_c Speed of the aircraft

V_j Velocity of the jet with respect to the tube

W_s Acoustic power of the stationary jet

W_v Acoustic power of the jet in motion

W_0 Reference acoustic power $W_0 = 10^{-12}$ watts

x Distance of a point in the plane of the tube, along the jet axis

x_i Coordinates along the axes i = 1,2,3

α Distance attenuation constant (3.1.3.4.)

α_i Exponent of S in the expression for the acoustic power within the octave i

β_i Exponent of V_j in the expression for the acoustic power in the
octave i

η Exponent of the convection factor

θ Direction from a point of observation with respect to the jet
axis

θ_M Direction of the maximum acoustic emission

$\psi(f)$ Acoustic power of a one-cycle band

ρ_a Air density

ρ_j Density of the gas in the jet

METHOD FOR THE DETERMINATION OF THE NOISE FROM TURBOJET AIRCRAFT ON TAKE-OFF TRAJECTORIES*

Michel Kobrynski**

ABSTRACT

The approximate determination of the maximum sound pressure of turbojet aircraft on the ground or in subsonic flight may be carried out from the laws of jet noise emissions using the generalized spectrum of the sound pressure and the directivity of the acoustic rays.

The first method is applicable when the jet Mach number is smaller than 2 (with respect to the velocity of sound in the atmosphere) and takes into account the theoretical variation of the acoustic power which is proportional to V_j^2, where V_j is the jet velocity. If the jet is in motion, as is the case in flight, the basic parameter is the difference $V_j - V_e$ of the jet and aircraft velocities.

In the second method, the vortex convection Mach number M_c and also, under some circumstances, the Mach number of the aircraft M appear in the correction factor

$$\left[1 - \left(M_c - \frac{M}{2} \right) \cos \theta_M \right]^{-1} \left(1 + M \cos \theta_M \right)^{-\eta},$$

where the exponent η and the emission angle θ_M of the maximum acoustic radiation are both functions of M_c.

This method is applicable for the prediction
of the noise of future airplanes such as the Concorde.
The Concorde turbojets will have a jet Mach number on
the order of 2.5 with respect to the speed of sound
in the atmosphere.

1. INTRODUCTION

By determining the noise produced by the take-off of aircraft
beforehand, it will be possible to define take-off conditions under
which the sound environment for people adjacent to airports is relatively
acceptable.

This study, which is already indispensable for present-day jet
aircraft, has acquired an increased importance due to the imminent
appearance of supersonic commercial transports.

These airplanes will be equipped with very powerful turbojets
and will cause an increase in the noise generated by the jets.

Even though the problem of determining the noise of future air-
craft has been the topic of investigation of researchers in different
countries, only a few publications on the subject have appeared. Coles
(Ref. 1) carried out an important experimental study of jet noise for
stationary jets and for the airplane Avon-Canberra in flight. This re-
sulted in curves showing the variation of the maximum sonic pressure
and the acoustic spectrum (by 1/3 of an octave) as a function of the
parameters of the jet for each case.

The object of this paper is to determine the laws which govern
the emission of sound of stationary and moving jets, to establish re-
lationships among them, and to propose a general method of calculation.
The latter is to be valid for standing aircraft as well as for aircraft
during taxiing and subsonic flight.

1.1 General Conditions

An aircraft flying over an observation point on the ground pro-
duces a sonic intensity at this point which varies as a function of
time. The analysis of the physical phenomenon observed in the case

---

* Numbers given in the margin indicate pagination in the original
   foreign text.
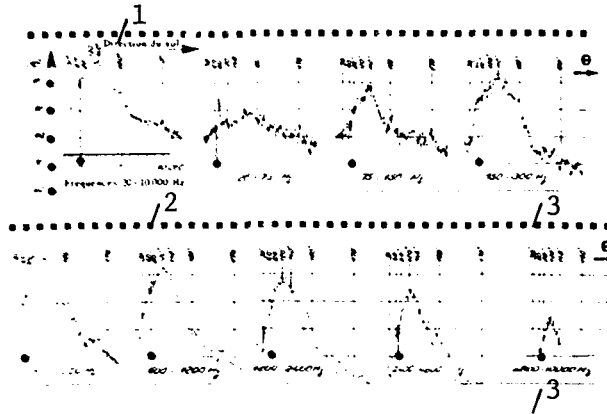
Figure 1

Aircraft Mirage IV. Sound Levels as a Function of Time.

Altitude: 190 m; Aircraft speed: 155 m/s; Speed of the jet: 540 m/s.

(1) Direction of flight; (2) Frequencies 20-10,000 cycles; (3) Cycles

of a jet aircraft is shown in Figure 1: These recordings show the variation of the total sonic level and of the level by octaves of frequency as a function of time, which is shown along the abscissa. The time 0, shown by a "tick" corresponds to the time at which the aircraft intersects the vertical at the point of measurement.

The angles at which the sonic waves are emitted indicate the characteristic direction of the noise; this is why the maximum is not observed when the aircraft is vertically overhead, that is to say, when the distance of the airplane to the point of observation is minimum and when one takes into account the time required for the sonic wave to reach this point.

Primarily the maximum values of sonic levels are significant, because then the effect of the noise is more pronounced. The prediction of aircraft noise can thus be based on the calculation of the maximum sonic levels.

The directivity of the noise is a function of the frequency band   /10 under consideration. It is not possible to simultaneously receive at one point maximum sonic levels for all frequency octaves (note that in Figure 1 there is a variable displacement of the maximum with

3
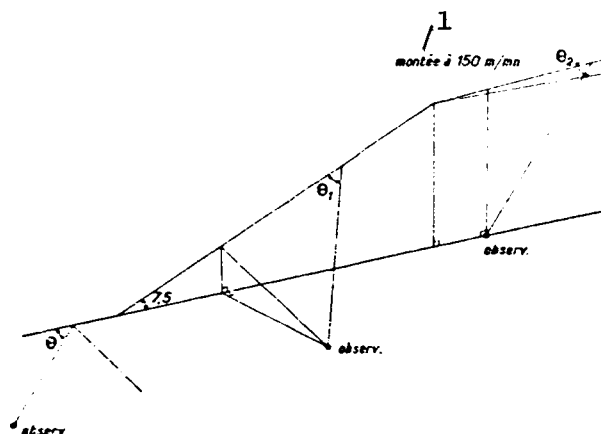
Figure 2

Take-off Trajectories for the Concorde

(1) Ascent at 150 m/mn

respect to the origin). The curve representing the total sonic level
does have a maximum, but this information cannot be used for the cal-
culation of the normalized audible perception, in pndb.

It has been generally accepted (ISO recommendation during the
course of normalization) that the maximum audible perception shall be
represented by the number of PNdB calculated with the successive maxima
within each frequency octave and not with simultaneous values.

The method of calculating the noise on the ground should therefore
make use of the laws governing sound emission of jets on the ground
(stationary jets) as well as those in the air, and also the direc-
tional characteristics of this emission. In addition, it should take
into account the relative positions of the sound sources and the ob-
servation points.

Figure 2 shows the characteristic points of the trajectory of an
aircraft such as the Concorde during a take-off: After the brakes are
released, there occurs a rolling phase on the ground, then a first as-
cent at full power which is followed by a second ascent, which is
somewhat less inclined and occurs under reduced thrust. Then the sound
on the ground diminishes.
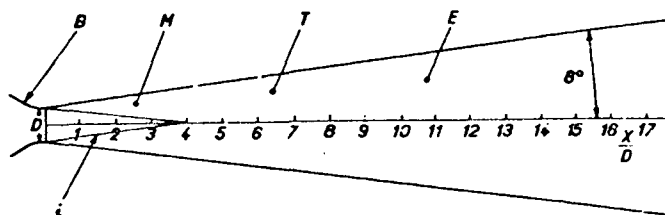
Figure 3

Outflow Geometry of a Jet

B – Nozzle; i – Potential outflow cone;
M – Mixing zone; T – Transition zone;
E – Completely turbulent zone.

It is desired to determine the sound on the ground below the track of the aircraft, as well as laterally, when the aircraft follows a trajectory of this type.

The experimental data used in this paper formed the conclusion of an effort carried out over several years. In order to be used, it was necessary to carry out an extensive analysis and numerous calculations. In this connection we would like to express our appreciation for the help of L. Avezard and J. Couratin, both members of the research group.

2. ACOUSTIC FIELD OF STATIONARY JETS

2.1. Definition of Velocities

The turbulence of a jet depends on the mach number and the Reynolds number of the outflow. In the aerodynamic sense, the jet is still considered to be subsonic and its velocity remains below the speed of sound within the fluid of motion which, in the case under consideration, is very hot.

The noise caused by the jet turbulence is radiated into the atmosphere, which is cold and stationary.

Let us set: V_j the expansion velocity of the jet, c_a the speed of sound in the outside atmosphere.
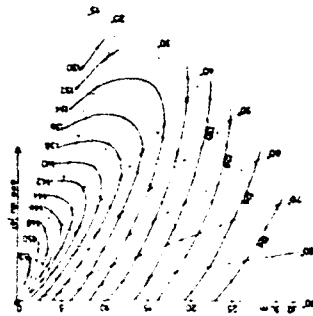
Figure 4

Turbojet Avon RA 29 R

Range 8,000 revolutions/minutes; Frequency
20 - 10,000 cycles; Curves of equal sonic
level (effective values).

We will set

$$M_j = \frac{V_j}{C_a}$$

This latter definition of the jet Mach number is used here.
A hot jet, which would be called subsonic in the sense of the first
paragraph, is already considered supersonic when V_j is still less
than the speed of sound in the jet, but larger than C_a.

At each point of the jet, the particles have an instantaneous
velocity which is random. The space-time correlation measurements
carried out by Laurence (Ref. 2) for a jet having a Mach number 0.3
and a Reynolds number of 6.10^5 showed that in the mixture zone (be-
tween the edge of the jet and the cone of potential outflow [Figure 3]),
the effective value of velocity fluctuations reaches 0.14 V_j, and in
this zone the average value velocity is on the order of 0.5 V_j.

The convective Mach number of the vortices is

$$M_c = 0.5 \frac{V_j}{C_a}$$

for a stationary jet.

2.2. Structure of the Acoustic Field

A jet exhausting into the atmosphere causes intense turbulence

Figure 5

Avon RA 29 R

Frequency 20 - 75 cycles.

(1) jet axis

in the shear layer with the ambiant air. This turbulence dissipates
a small fraction of the kinetic energy of the jet in the form of
noise and it is sufficiently large for the noise to become extremely
intense.

Figure 3 shows the mixture zone between the cone of potential
outflow and the atmosphere. The amount of turbulence which develops
increases linearly with the distance x to the apex of the cone within
this zone. In this zone, the vortices are carried along at the con-
vection speed $M_c C_a = 0.5\ V_j$.

Outside of this mixture zone, which extends to a length of 4 to
5 diameters D of the nozzle, the turbulence ceases to increase and
its velocity decreases as $\frac{4}{x}$, for $\frac{x}{d} > 8$.

Dimensional considerations (Ref. 3) allow one to attribute
about one-half the acoustic power generated by the jet to the mixture
zone. In addition, the acoustic power emitted by each ring of the
jet remains constant (x law).

The different parts of the jet emit sound in different frequency
bands. The characteristic frequency is proportional to V_j/x. Near
the orifice, the emitting rings cause a spectrum which is predominantly
shrill. The low frequencies appear much more downstream.

The distribution of the acoustic energy in the atmosphere,

7
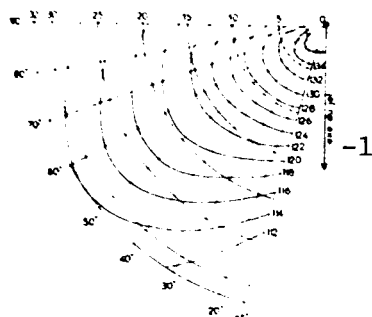
Figure 6

Avon RA 29 R

Frequency 4800 - 10,000 cycles

(1) jet axis
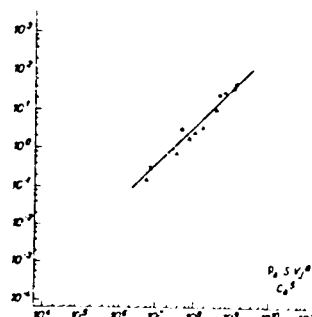
Figure 7

Stationary Jets, Acoustic Power as a Function of the Lighthill Parameter

Δ Turbojet Avon RA 21 R
● Turbojet Avon RA 29 MK 522
0 Turbojet ATAR 9 K5
× Turbojet Marboré II

according to the theory of Lighthill (Ref. 3), follows the emission of acoustical quadruplets equivalent to the jet. A quadruplet (source of order 2) consists of the association of four zero order sources which, associated in pairs, form two dipoles having opposing phase. The acoustic field of the quadruplet is characterized by 4 lobes separated by 2 nodal lines which intersect at a right angle and are oriented at 45° with respect to the axis of the jet. Thus, they occur along the direction of maximum perturbations due to fluctuations of the shear layer between the fluid in motion and the atmosphere. /12

The structure of the acoustic field of the jet is shown in Figures 4 to 6. We show curves of equal acoustic pressure in a plane passing through the axis of the jet. Figure 4 shows isobaric curves for all audible frequency intervals from 20 to 10,000 cycles. Figure 5 corresponds to low frequencies, and Figure 6 to shrill frequencies.

The orientation of the isobar system allows one to locate the apparent positions of emitting sources distributed over the body and the outflow. It also gives an account of the characteristic directions of the acoustic field.

8

It can be seen that the sources corresponding to low frequencies are located very far downstream from the outflow. On the other hand, the origin of the high frequencies is very close to the nozzle. In all cases, the direction of maximum acoustic radiation is oblique with respect to the axis of the jet, as the theory of quadruplets indicates.

The acoustic radiation of the quadruplets must be symmetric, not only with respect to the jet axis, but also with respect to a plane normal to this axis. In other words, it must be possible to observe the same lobes along the downstream and upstream directions. The form of the experimental isobars does not confirm this.

Lighthill (Ref. 4) attributes the absence of the rear lobes (secondary lobes) to convection effects of the quadruplets, in a high velocity jet with average local speed $M_c C_a$: The quadruplets, which have become mobile, are deformed in such a way that the oblique lobes are extended along the direction of displacement of the jet and are shortened in the opposite direction. This terminates the quasi-disappearance of the secondary lobes.

This important effect and its consequences have been taken into account in this paper (see Chapter 4), but it is necessary to first study the jet noise with the hypothesis of "solid" quadruplets (jets which have an average velocity that is not too high), first neglecting this convection effect. It will be introduced later.

3. CALCULATION OF MAXIMUM ACOUSTIC PRESSURE LEVEL OF JETS, INDEPENDENT OF THE EFFECT OF THE CONVECTION VELOCITY OF VORTICES

3.1. Stationary Jets

The calculation of maximum acoustic pressure N_s introduces the acoustic power of the jet, the generalized spectrum of the acoustic power and the indices of maximum directivity of acoustic pressure levels.

3.1.1. Acoustic Power of Jets

3.1.1.1. Law of Lighthill

The calculation of the acoustic power emitted by a subsonic (with respect to C_a) stationary jet can be carried out by

means of a dimensional analysis of sound having aerodynamic origin coupled with experimental research.

Lighthill (Ref. 3) studied the laws of acoustic emission of a turbulent outflow of small Mach number. He showed that a vortex element v_t causes an acoustic power proportional per unit of volume of turbulence equal to

$$\frac{v_t \, f^4 \, \overline{T^2}}{\rho_a \, c_a^5}$$

f is a characteristic frequency of turbulent fluctuations. $\overline{T^2}$ is the mean squared value of the intensity of the quadruplet T_{ij}. The tensor T_{ij} is approximately given by

$$T_{ij} \approx \rho_a V_i V_j \qquad i, j = 1, 2, 3$$

V_i is a characteristic velocity of the vortex depending on x_i.

In the mixture zone of the jet (Figure 3) with the characteristic velocity V, it is assumed that the term $\rho_a V_i V_j$ has the dimension $\rho_a V^2$.

Let us write $\overline{T^2}$ in dimensional form and let us consider the volume V_i within which the turbulent effects are produced. The acoustic power will then be proportional to

$$\rho_a v_t V_t \, f^4 V^4 / c_a^5$$

L is a characteristic length of the turbulent zone.

For the entire jet we may introduce the similarity laws $v_t \sim L^3$ $L^2 \sim S$, where S is the ejection area of the gases, and $\rho \sim V/L$.

Using these relationships, the acoustic power of the jet W_s is proportional to

$$\rho_a \, S V^8 / c_a^5$$

Let us introduce the coefficient of proportionality K. As the characteristic velocity for V, we introduce the expansion velocity of the jet V_j. We have

$$W_s = K \frac{\rho_a \, S V_j^8}{c_a^5}$$

$$(1)$$

10

The coefficient K varies as a function of the turbulence of the jet between 3.10^{-5} and 1.10^{-4}. The first value is usually assumed.

When the jet is warm, equation (1) becomes

$$W_s = K \; \frac{\rho_j^2 \, s \, v_j^3}{\rho_a \, c_a^5} \tag{2}$$

where the volume density of the gases is p_j.

In any case, for turbojets which operate without reheating of the gases, the acoustic power emitted can be determined by the simpler formula (1), and which is used in this paper.

The acoustic power is usually expressed by means of an acoustic source on the logarithmic scale. The acoustic power level N_W is then given by

$$N_W = 10 \; log \; \frac{W}{W_o} \tag{3}$$

W_o is the reference power 10^{-12} watts (*).

The acoustic power level of the jets is given by:

$$\tag{3}$$

where

$$\begin{cases} N_w = 10 \; log \; K \; \dfrac{\rho_a \, S \, v_j^g}{C_a^5 \, 10^{-12}} \quad dB_p \\[2mm] K = 3.10^{-5} \end{cases}$$

$$N_w = 10 \; log \; (3 \, 10^7 \, \rho_a \; \frac{S \, v_j^3}{C_a^5}) \quad dB_p \tag{4}$$

The quantities are expressed in M.K.S. units.

_____

(*) Anglo-saxon papers often use $W_o = 10^{-13}$ watts due to the fact that they express acoustic intensities in W/sq ft and not in W/m^2, and because 1 m^2 $\sim$ 10 sq ft.

3.1.1.2. Experimental Verification

We measured the distribution of the acoustic pressure levels around the following turbojets: ROLLS-ROYCE RA 29 MK 522, RA 21 R, MARBORE II, and ATAR 9 K 5. These turbojets are of the direct flux type and their tail pipes are not equipped with jet silencers. The conditions encountered do lend themselves to an experimental verification of the Lighthill formula.

For each operational regime, the acoustic power caused by the jet was calculated by integrating over a hemisphere having a large radius and which surrounds the jet. The conditions of the acoustic far field were used.

Figure 7 shows the results obtained as a function of the parameter $Pa \dfrac{SV_j^8}{c_a^5}$, in logarithmic coordinates.

In this representation, the average variation of the acoustic power has the slope 1, which verifies the fact that the V_j^8 is satisfied. According to equation (1), the coefficient K equals 3.10^{-5}.

3.1.1.3. Acoustic Power of Jets in Groups

Commercial jet aircrafts are always propelled by jets in groups. It is therefore necessary to determine the total acoustic power level emitted by n identical turbojets functioning in the same regime.

Assuming that there is not significant interference between the acoustic fields of the adjacent jets, the total acoustic power level is given by a simple law of addition of the effects of each one, i.e.,

$$N_T = N_w + 10 \log n \quad dB_p$$

(5)

This relation will be adopted for aircraft in flight. In the /16 stationary case, the effect of grouping causes an increase in the acoustic power level, which is experimentally given by $10 \log n^{\frac{1}{2}}$. When the grouping of the turbojets is "locked", the total acoustic power seems to increase less rapidly than would be expected from the terms $10 \log n$ or $10 \log n^{\frac{1}{2}}$.

12

3.1.2. Spectrum of the Acoustic Power of Jets

3.1.2.1. Definition of the Generalized Spectrum

Experience shows that the acoustic power of jets is proportional to SV_j^8, according to the theory of Lighthill. In spite of this agreement, it is remarkable that no portion of the acoustic power spectrum obeys the law SV_j^8. This can be shown by the examination of the generalized spectrum of acoustic power. In effect, due to the large diversity in the dimensions of jets, and in the gas velocities encountered during the investigation, it is logical to look for a representation of the power spectrum as a function of quantities that have no dimensions (Ref. 4).

Let $\psi(f)$ be the acoustic power of the jet associated with each band one cycle wide at the frequency f: The total power will be the integral $W_s = \int_{\ell_4}^{\ell_2} \psi(f)df$ between the limits $f_1 f_2$, which, for example, can be the extremes of the audible range.

The nondimensional ordinate chosen for representing the generalized spectrum is the logarithmic value

$$10 \log \frac{\psi(f)}{W_s} \frac{V_j}{D} = 10 \log \psi(f) - (10 \log W_s - 10 \log \frac{V_j}{D}) \tag{6}$$

and its abscissa is the Strouhal number $\frac{fD}{V_j}$. These quantities are independent of the units chosen because V_j/D has the dimension of a frequency.

3.1.2.2. Experimental Determination of the Generalized Spectrum

In the case where measurements were analyzed by frequency bands, whose cutting-off frequencies were f_i, $f_i + 1$ and the bandwidth $\Delta f_i = f_{i+1} - f_c$, the frequency f under consideration is the geometric mean $f_c = \sqrt{f_i \cdot f_{i+1}}$. The spectropower level for the frequency $f = f_c$ is given by

$$10 \log \frac{\psi(f)}{W_s} = N_{wc} - 10 \log \Delta f_c \tag{7}$$

N_{wc} is the acoustic power in the band f_i, f_{i+1} (in the case of the

13
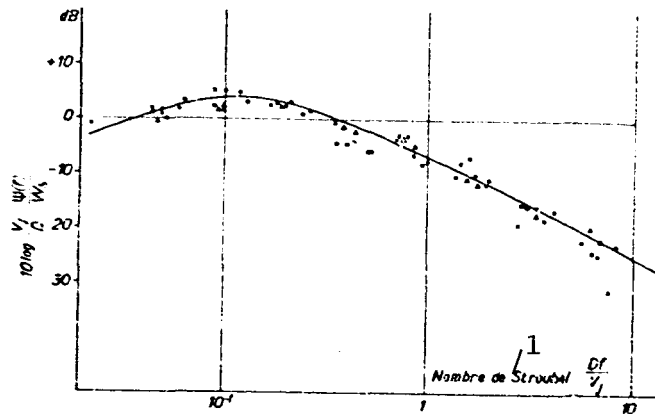
Figure 8

Stationary Jets, Generalized Spectrum of Acoustic Power

Δ Turbojet Avon RA 21 R   0 Turbojet Avon RA 29 MK 522
0 Turbojet ATAR 9 K5   × Turbojet Marboré II

(1) Strouhal number.

octave band, $f_{n+1} = 2 f_n$, $f_c = f_n \sqrt{2}$, $\Delta f_n = f_n$).

The results of calculations carried out in this way for a large /17
number of turbojet acoustic power measurements are plotted in
Figure 8 as a function of coordinates without dimension. These points
allow one to construct an average curve corresponding to the generalized
spectrum which characterizes stationary jets and which are subsonic
with respect to the speed of sound in the jet (see 2.1.). This experi-
mental curve shows a rounded maximum for a Strouhal number in the
vicinity of 0.1. Above this, the curve tends to follow the theoreti-
cal one which decreases according to f^{-2} (Ref. 6).

3.1.2.3. Variation of the Acoustic Power by Octaves as a Function of D and V_j

By assigning variable values to D and V_j, the curve
representing the generalized spectrum allows one to determine the varia-
tions of the acoustic power spectrum as a function of these variables
If this calculation is carried out for the eight frequency octaves in
general use, one finds that at the low frequencies the acoustic power
varies as $S^{2 \cdot 2} V_j^6$. At the high frequencies, it varies as $S^{0 \cdot 3} V_j^3$, and

14

the total power varies according to SV_j^8 (3.1.1.1.).

The acoustic power within each octave i is therefore of the form $S^\alpha V_j^{\beta i}$, and the exponents are given in the following table and were compiled according to our experience:

TABLE I

EXPONENTS OF S AND V_j OBTAINED FROM

THE GENERALIZED SPECTRUM WHEN THE
TOTAL ACOUSTIC POWER IS PROPORTIONAL
TO SV_j8

Octave No.	Frequency Band Cycles	Surface Exponent s	Velocity Exponent V_j
1	20-75	2,2	6,0
2	75-150	1,75	7
3	150-300	1,25	7,5
4	300-600	1	8,5
5	600-1200	0,8	8,5
6	1200-2400	0,5	9
7	2400-4800	0,4	9
8	4800-10000	0,3	9
Total	20-10000	1	8

These results confirm the conclusions of an earlier study (Ref. 7). <u>/18</u> One establishes a satisfactory agreement with theoretical studies of Powell (Ref. 6). This author analyzes the form of the acoustic spectrum of jets and shows, using similarity conditions, that the low frequency spectrum (emitted by the zone downstream from the cone of constant velocity) has the dependence $S^{2.5}V_j^5f^2$. For the high frequencies (emitted by the mixture zone, near the nozzle), it varies according to $F^{0.5}V_j^9f^{-2}$.

According to this theory, the form of the acoustic power spectrum of the jets will be triangular and symmetric (in a logarithmic representation as a function of frequency). The slopes will be f^2 and f^{-2}, respectively.

3.1.2.4. Calculation of the Acoustic Power by Octaves of Frequency

If the quantities D and V_j of a jet are known, the expressions 1 and 3 give the total power level N_W. The curve shown in Figure 8 results in an ordinate, k_i, and which is equal to expression (6) for each frequency f. According to (3) and (7), expression (6) is equal to

$$k = 10 \log \frac{Y(f)}{W_o} - \left(10 \log \frac{W_t}{W_o} - 10 \log \frac{V_j}{D}\right)$$

$$= N_w - 10 \log \Delta f - N_w + 10 \log \frac{V_j}{D}$$

where

$$N_{w} = N_w + 10 \log \Delta f - 10 \log \frac{V_j}{D} + k \qquad (8)$$

k_i, positive or negative, is the number of decibels read along the ordinate of the curve of Figure 8 for the abscissa $\dfrac{Df_c}{V_j}$

f_c is the central frequency of the band being analyzed.

The values of k and $10 \log \Delta f_i$ are shown in Table II for the eight common frequency bands.

TABLE II

MEAN GEOMETRIC FREQUENCY AND VALUE OF
10 log Δf_i FOR EACH OCTAVE

/19

Octave No.	Frequency Band Cycles	Mean Geometric Frequency fc	$10 \log \Delta f$ dB
1	20-75	53	17
2	75-150	106	19
3	150-300	212	22
4	300-600	425	25
5	600-1200	846	28
6	1200-2400	1693	31
7	2400-4800	3380	34
8	4800-10000	6880	38

16

3.1.3. Maximum Acoustic Pressure

Our goal in the calculations is to find the maximum acoustic
pressure, both the total one and by frequency octaves. Since the
acoustic power (total and by octaves) has been determined by the pre-
ceding calculation, we will now calculate the average acoustic pressure
level at a given distance, such as would be observed if the acoustic
sources were omni-directional. Then we will treat the case where the
index of directivity varies according to the angle of emission and
modifies the distribution of this pressure in space. In particular,
we seek the level corresponding to the angle of maximum emission.

3.1.3.1. Average Spatial Acoustic Pressure

As a beginning, let us calculate the distribution of
the acoustic powers, N_W and N_{W_i}, along a hemisphere of radius r,
centered at the emitting source, assuming that this acoustic power is
emitted by a zero order, omni-directional emitter (equivalent to a
pulsating sphere).

Under these conditions, the average acoustic intensity I_m trans-
mitted per unit of surface along the radial direction is equal to

$$I_m = \frac{W_s}{2 \pi R^2}$$

The acoustic pressure level N_m is given by   /20

$$N_m = 10 \log \frac{I_m}{I_o}$$

I_0 is the reference intensity equal to 10^{-12} watts/m^2. Thus

$$N_m = 10 \log \frac{W_s}{10^{-12}} - 20 \log r - 10 \log 2\pi$$

or from (3)

$$N_m = N_w - 20 \log r - 8 \quad dB \tag{9}$$

N_m is the acoustic pressure level with respect to the reference level of
$20\mu Pa$, and r is expressed in meters.

The average pressure level by octaves N_{m_i} can be calculated like-
wise by replacing N_W by the value N_{W_i} of the corresponding octave.

However, this is only exact when the additional attenuation of the

17
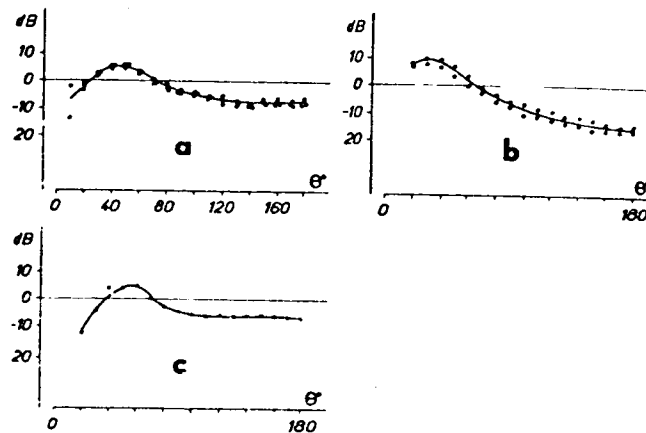
Figure 9

Stationary Jets, Directivity Index.   Frequency 20 - 10,000 Cycles.

a - AVON RA 29 MK 522; b - ATAR 9 K5; c - Marboré II

acoustic waves at the time of their propagation in the atmosphere (molecular attenuation) remains negligible.   In practice, this latter effect remains very small, even though it depends on wavelengths, for all audible frequencies and for a distance of 30 m, for example.   This distance is sufficiently large with respect to the wavelengths involved. For r = 30 m, we have

$$\begin{cases} N_{n} = N_{w} - 37.5 \ dB \\ N_{n_{L}} = N_{w_{L}} - 37.5 \ dB \end{cases} \tag{10}$$

3.1.3.2.   Directivity Index

It is known (Ref. 3) that the acoustic field of a jet can be represented by the field of a system of acoustic quadruplets. These second order emitters cause an anisotropic acoustic field.   It is therefore necessary to apply corrections to the mean acoustic spatial level to take into account the directional properties of the acoustic radiation of the jet.   This correction, which leads one to the maximum value of acoustic pressure, is the directivity index, I. D.:

$$I.D. = 10 \ \log G (\theta) \ dB$$

$Q(\theta) = \frac{P^2(\theta)}{P_m^2}$ is the directivity factor,

P(θ) is the acoustic pressure in a direction corresponding to the angle θ and at a given distance,

P_m is the average pressure at the same distance.

The directivity index is positive or negative depending on whether the acoustic pressure for a given angle θ is larger or smaller than the average acoustic pressure at the same distance (the angle θ is measured from the axis of the jet).

This index is given in dB by:

$$I.D. = 20 \log P(\theta) - 20 \log P_m$$

or, using our notation:

$$I.D. = N(\theta) - N_m \ dB \tag{11}$$

N(θ) is the acoustic pressure level associated with the azimuth θ.

Combining the relationships (10) and (11), we have, for r = 30 m:

$$N(\theta) = N_w + (I.D.)_t - 37.5 \ dB \tag{12}$$

for the total noise level and

$$N_i(\theta) = N_{w_i} + (I.D.)_i - 37.5 \ dB \tag{13}$$

for that of the octave i (i = 1, 2 ..... 8).

Figures 9 and 10 show an example, for the ATAR, of experimental curves of the mean variation of the directivity index as a function of the angle θ. The following table shows the maximum directivity indices for the frequency intervals 20-1000 cycles and by octaves. These were obtained as the average of many measurements:

TABLE IIIMAXIMUM DIRECTIVITY INDICES OF TURBOJET JETS.
DISTANCE FROM 30 TO 60 m.

Frequency Band Cycles	I.D. max dB
20-10000	6
20-75	7
75-150	7
150-300	6
300-600	6
600-1200	5
1200-2400	4
2400-4800	4
4800-10000	4

3.1.3.3. Maximum Acoustic Pressure of Stationary Jets

The calculation of the maximum acoustic pressure of stationary jets (total level and level by frequency octave) is carried out by a series of quite laborious steps. If one desires only the pressure level value in the direction of maximum emission, it is possible to draw graphs which will give this result directly.

The lines shown in Figures 11 and 12 correspond to calculations of the maximum acoustic total levels (N_s) and the maximum levels by frequency octave (N_{si}), as a function of the expanded jet. The calculations were carried out for a difference of 30 m from the output nozzle.

The same figures show the results of measurements carried out with the turbojets ROLLS-ROYCE AVON RA 29 MK 522, ATAR 9K5, VERDON, MARBORE II and PALAS. The surface S of the nozzle of these turbojets varies between 0.2705 m^2 (ATAR) and 0.0155 m^2 (PALAS), which is a ratio of 17 to 1. This is why the measured acoustic levels were corrected by the term $10 \log \left(\frac{S}{S_o}\right)^{\alpha}$, where S_o is a reference surface, 0.2215 m^2 (AVON), and α is the exponent given by Table I. (For the time being, we neglected the effect of the variation of the volume mass of the expanded jet, because the effect on the acoustic levels of the turbojet operating without afterburner is small.*)

Remark: More complete values, as a function of the hygroscopic degree, are presently being standardized by the I.S.O.

* This paramter is introduced in a publication written after this one (Ref. 20).

20
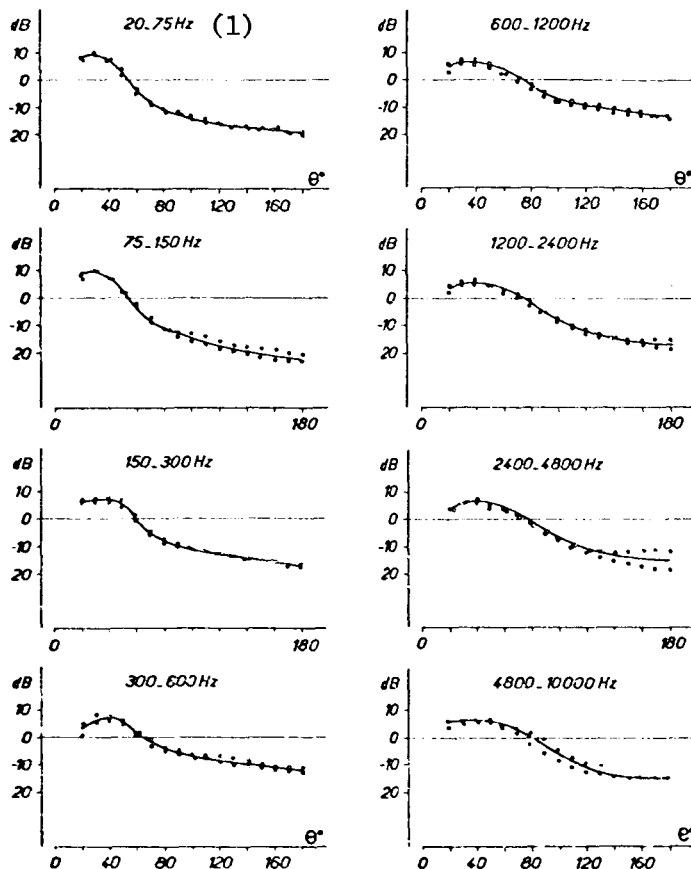
Figure 10

Stationary Jets.   Directivity Index for the 8 Frequency
Octaves (ATAR 9 K5).

(1) Cycles

The choice of a reference distance leads one to apply a second
correction to the measurements in the form of the term $10 \log \left(\dfrac{r}{r_o}\right)^2$,
where r is the radius of the circle adapted for the various experiments
and r_o = 30 m. This term represents the geometric attenuation given
by the law $1/r^2$. An examination of Figures 11 and 12 shows that the

21
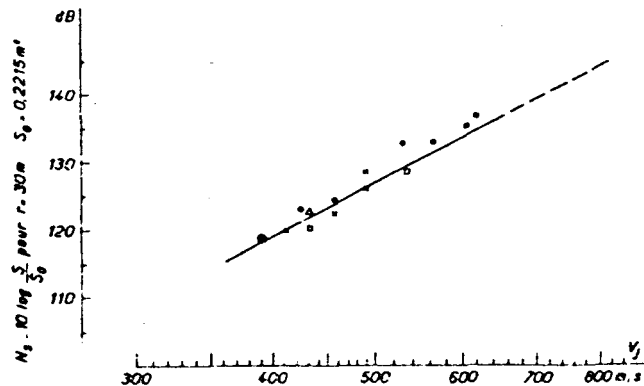
Figure 11

Maximum Sonic Levels as a Function of the Speed of the
Jet. Frequency 20 - 10,000 Cycles.

—— Mean curve SV_j^2; ● R. R. AVON RA 29 MX 522;

Δ Verdon; O ATAR 9 K5; × Marboré II; ● Palas; □ Derwent.

agreement between the theoretical predictions and the measurements is
reasonably satisfactory ($\pm$ 3 dB).

However, these results are not valid except for a short distance
from the turbojet, for the atmosphere attenuation remains negligible.
At larger distances, it is necessary to examine these attenuation laws.

3.1.3.4. Attenuation Laws of Acoustic Radiation with Distance

An acoustic source radiating into a homogeneous un-
limited space produces the intensity I_r at a point situated at the dis-
tance r:

$$I_r = (1/r^2) I_4 e^{-r}$$

where I_1 is the intensity received in the same direction at the distance
unity, and α is an attenuation constant depending on the characteristics
of the atmosphere.

The total attenuation in decibels between the distances r and r_0

22
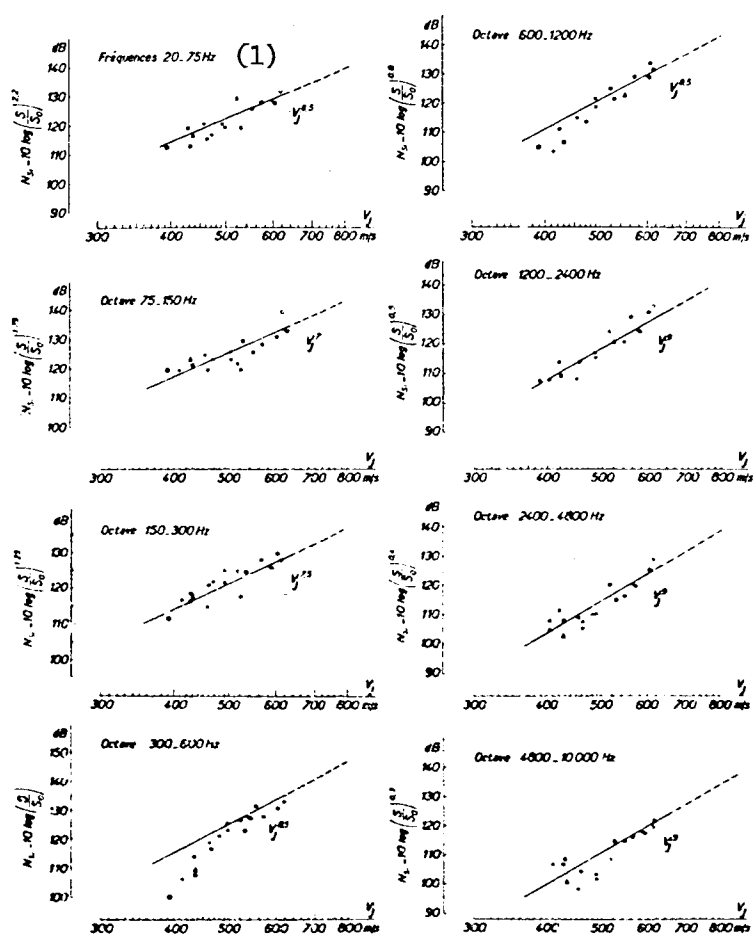
Figure 12

Maximum Sonic Levels by Octaves as a Function of the
Speed of the Jet

—— Calculated lines; ● R.R. AVON RA 25 MK 522;
Δ Verdon; O ATAR 9 K5; × Marboré II; ● Palas;
□ Derwent.

(1) Cycles

is thus given by

$$A = 20 \log \frac{r}{r_0} + 10 \alpha (r - \varsigma) \log e \quad dB \qquad (14)$$

The first term is the geometric attenuation due to propagation.

23
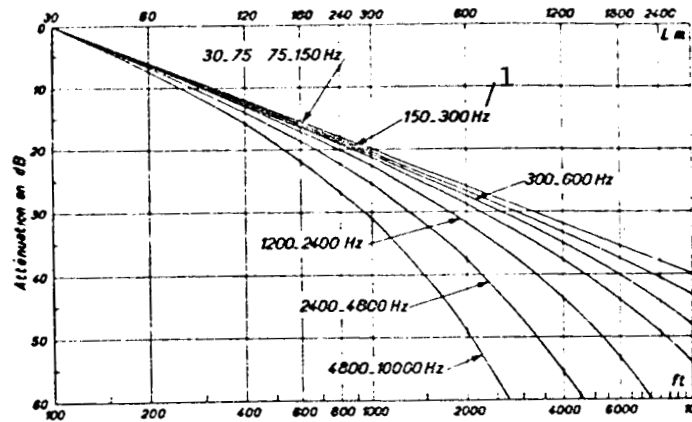
Figure 13

Attenuation of Pressure Sound Levels as a Function of
the Distance of Air to Ground Propagation

Standard atmosphere, temperature 15°, relative humidity 50%.

(1) Cycles

The attenuation in decibels due to atmospheric absorption (second term of
equation (14), above) was determined by Wiener (Ref. 8) as a function of
the frequency octaves for a temperature of 15° and a hydroscopic state
of 50%. It is expressed as the loss in decibels for a distance of 300 m.

<div align="center">TABLE IV</div>

ATTENUATION OF THE SOUND OVER 300 m FOR THE AMBIANT TEMPERATURE
OF 15°C AND THE HYGROSCOPIC STATE OF 50%

Fre-quency	Attenuation dB /300 m
20–75	0,16
75–150	0,16
150–300	0,33
300–600	0,70
600–1200	1,50
1200–2400	3
2400–4800	6
4800–10000	12

Figure 13 shows the grid of attenuation curves calculated from this

24
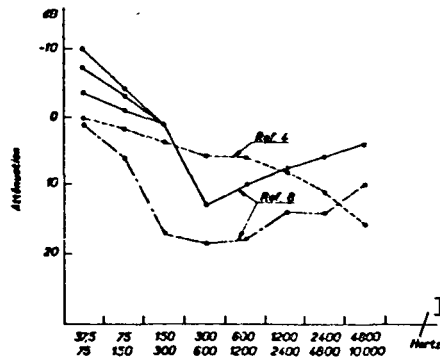
Figure 14

Attenuation of Acoustic Waves Near the Ground,
Measured and Calculated. For a Distance of 100 to 1400 Feet
From the Source.

––––– Measured at London Airport; –·– Measured at Radlett;
––– Calculated.

(1) Cycles

expression (14) at distances between 30 and 3000 m.

Let us now assume an acoustic source radiating near the ground:
An image source appears, and the measurement point, which is also located
near the ground, will receive a reflected wave in addition to the direct
acoustic wave. This is why the acoustic power of stationary jets is
calculated by integration of the acoustic energy over a half-sphere
centered at the acoustic point.

We will assume that the distance between the point of reception
of the noise and the source is large, so that the conditions of the
acoustic far field prevail (distance is large with respect to the wave
lengths, thus the geometric attenuation due to propagation follows the
law $1/r^2$). The attenuation constants due to the atmosphere and the
ground can be calculated as a function of distance when the meteorologi-
cal parameters are fixed and under the assumption that the ground has a
fixed characteristic inpedance.

In practice, this impedance varies depending on the nature of the
ground: concrete runway, sandy terrain or prairie, and the reflections
of the acoustic waves on the ground can be either total (concrete) or
partial (porous ground).

25
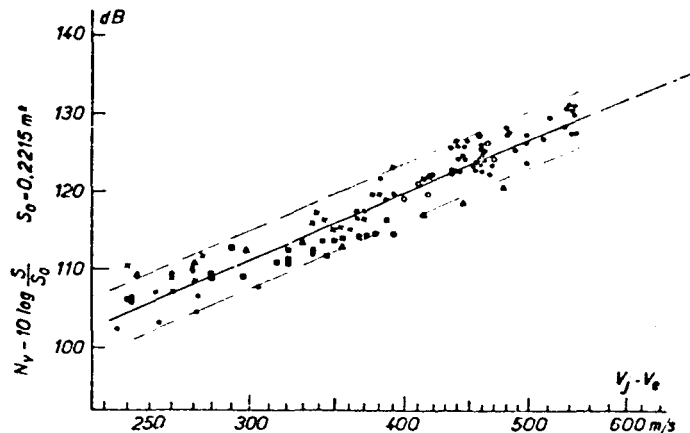
Figure 15

Aircraft in Flight. Maximum Sonic Levels as a
Function of Jet Velocity with Respect to the Atmosphere

Corrected altitude 30 m, Frequency 20 - 10,000 cycles.
(1 Turbojet)

● Caravelle; 0 Mirage IV; × Fouga; ■ Gloster Meteor;
▲ Mystère IV A

The problem of sound propagation close to the ground was examined
in England and in the United States. This work is presently still being
carried on. Greatrex (Ref. 8) published results obtained for
the ground near Radlett and London Airport (Figure 14). In these two
cases, the attenuation was measured by frequency octaves when the point
of reception of the noise passed from 100 to 1414 feet (30 m to 430 m). /25
The sound sources were a Boeing 707-420 and a Comet, operating at a
fixed point. It was found that for the same distance between the source
and the receiver, there was a difference on the order of 7 dB
between the two series of the experiments.

The same figure shows the attenuation calculated from the ground-
ground propagation curves given by Cole (Ref. 5). There is a noticeable
difference with respect to the English data. It can be seen that
phenomena due to ground effects are complex.

3.2. Jets in Motion

When a jet having the velocity V_j (with respect to the nozzle)
operates from an aircraft in flight, which itself has a somewhat smaller
speed, $-V_e$ (measured in the direction opposite to V_j), with respect to

26

the air, the outflow can be referred either to axes fixed with respect
to the aircraft,or axes related to the atmosphere. Since acoustic phe-
nomena are studied in this atmosphere, which on the average is fixed,
it is logical to consider the absolute velocity of the jet, $V_j - V_e$.

3.2.1. Total Maximum Acoustic Pressure of Aircraft in Flight

We carried out 100 recordings of the acoustic pressure caused
by the passage of various types of aircraft (Table V), for jet velocities,
V_j, between 320 m/s and 620 m/s and aircraft velocities, V_e, between
55 m/s to 255 m/s. The aircraft passed vertically over the measurement
microphones.

TABLE V

AIRCRAFT TYPE

Aircraft	Turbojets	Gas Ejection Surface m^2
Mirage IV	ATAR 9K5	0,2780
Caravelle, stage I	AVON RA 29, RK 522	0,2215
Mystère IV A	VERDON	0,2705
FOUGA	MARBORE II	0,0370
Gloster-Meteor	DERWENT	0,1295

The analysis carried out by frequency octaves as a function of time <u>/26</u>
made it possible to determine the maximum acoustic pressure levels. The
obtained values of N_{vj} were corrected for an overflight altitude of 30 m,
using the curves shown in Figure 13 and in order to make the effect of
molecular attenuation negligible. These results were used for the cal-
culation of the maximum total acoustic levels N_v.

The obtained values were reduced by 3 dB, except for the Mystère IV A,
which has a single engine (see 3.1.1.3.).

It should be noted that the acoustic levels can be determined to an
accuracy of $\pm$ 4 dB by means of the empirical formula

$$N_v = 10 \log S \left(\frac{M_j}{1+M}\right)^{10} + 119 \text{ dB}$$

In another representation, the acoustic levels N_v are referred to
the reference surface $S_0 = 0.2215$ m^2 and the results obtained are shown
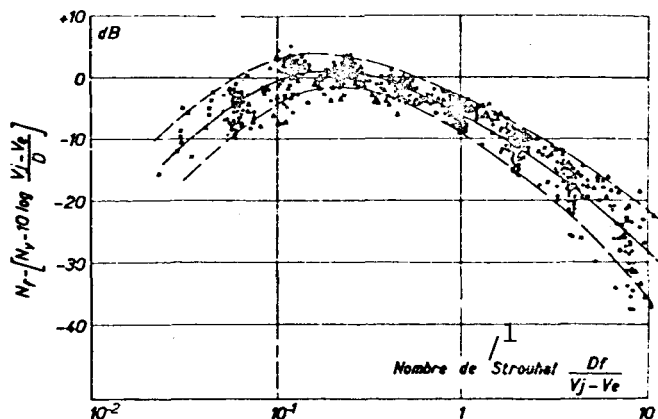
Figure 16

Aircraft in Flight. Generalized Spectrum of Maximum
Sonic Pressure

Corrected Altitude 30 m.

● AVON RA 29 MK 522; ■ Derwent; O ATAR 9 K 5; ▲ Verdon;
× Marboré IV

(1) Strouhal number

as a function of the jet velocity relative to the atmosphere, $V_j - V_e$
(Figure 15).

3.2.2. Generalized Spectrum of the Maximum Acoustic Pressure Levels

The acoustic spectrum of jets in motion received on the
ground depends on the velocity of the aircraft, V_e, and, just as in the
case of stationary jets, the performance numbers of the turbojets, the
diameter of the jet, and, due to molecular attenuation, the altitude
of the overflight.

Since we have established that, for aircraft in flight, the total
noise level depends on the velocity of the jet, referred to the atmosphere,
it can be assumed by analogy that the frequencies which appear F_a, and
which are received on the ground also depend on the difference $(V_j - V_e)$.

With this hypothesis, the generalized spectrum of the maximum
acoustic pressure level of jets in motion can be represented using the
following coordinates:

28

as abscissa — $\frac{D}{V_j - V_e} f_i$

as ordinate — $N_f - [N_v - 10 \log \frac{V_j - V_e}{D}]$ $\Bigg\}$ (15)

N_f is the spectroacoustic pressure level which, for the octave with the index i, is given by

$$N_f = N_{v_i} - \log \Delta f_i$$

The results obtained (Figure 16), enable us to compile a /27 curve of average variation of the generalized spectrum of the maximum acoustic pressure level of aircraft in flight.

3.2.3. Method of Calculating the Maximum Acoustic Pressure Levels of Aircraft in Flight

Let us assume a double jet, for which is known the velocity V_e, the jet velocity V_j, the gas exit surface area S, and the vertical altitude from a point on the ground. It is necessary to determine maximum acoustic pressure levels N_v for the interval 20-10,000 cycles and the acoustic pressure levels by frequency octaves, N_{v_i}.

The value of N_v for an altitude of 30 m is known from Figure 15 as a function of $V_j - V_e$. The generalized spectrum shown in Figure 16 makes it possible to calculate the values of N_{v_i} by octaves. Finally, the curve in Figure 13 will give the necessary corrections as a function of the altitude in question. The values of N_v found in this way allow one to compute the normalized audible level in P.N. dB.

For relative jet velocities between 250 m/s and 550 m/s, the accuracy of this method is $\pm$ 4 dB, which is quite satisfactory.

For larger values of $V_j - V_e$, the calculation is still possible if we allow a variation of N_v as a function of the speed of the jet with respect to the atmosphere. It is continued in such a way that it follows the empirical law given by the line shown in Figure 15.

This hypothesis remains to be verified.

3.3. Limits of Validity of the Variation of the Acoustic Power According to $V_j{}^8$

In a paper devoted to the study of jet noise (Ref. 7), it was shown

29

that the acoustic efficiency (ratio of the total acoustic power to the mechanical power of the jet) is proportional to $M^{4 \cdot 5}$. This leads to an efficiency of 10^{-4} for $M_j = 1$ and of $3 \cdot 10^{-3}$ for $M_j = 1.7$.

The study of rocket noise (Ref. 10) shows, on the other hand, that for Mach numbers M_j in the vicinity of 7, the acoustic efficiency does not surpass $7.5 \cdot 10^{-3}$.

It is remarkable that the acoustic efficiency reaches this order of magnitude even for turbojets functioning with afterburners, such as the ATAR 9 K 5, where the Mach number M_j is only 2.5.

The fact that the acoustic efficiency of jets strives toward a limit at the high velocities shows that the acoustic power cannot always increase according to a single $V_j{}^8$-law.

The study of this question, which is necessary for faster jets, such as those of the Concorde, will be carried out in the next chapter.

4.   CALCULATION OF THE MAXIMUM ACOUSTIC PRESSURE
     OF JETS, BASED ON THE EFFECT OF VELOCITY
     CONVECTION OF VORTICES

4.1.   Stationary Jets

4.1.1.   Directional Distribution of Acoustic Intensity

Lighthill showed (Ref. 4) that an instantaneous pressure P is associated with each acoustic quadruplet. At a point a distance r from this source, which is in motion in a jet, the instantaneous pressure P in the direction θ is given by

$$P - P_0 = \frac{x_i \, x_j \, \ddot{T}_{ij}\left(t - \frac{r}{C_a}\right)}{4\pi \, r^3 (1 - M_c \cos\theta)^3} \tag{16}$$

T_{ij} is the characteristic tensor of the quadruplet.

P_0 is the static pressure and $\sqrt{(P - P_0)^2}$ is the effective pressure, emitted at the time $\left(t - \dfrac{r}{C_a}\right)$.

The effect of convection enters only by means of a factor $(1 - M_c \cos\theta)^{-3}$, which increases the acoustic radiation of motion of the sources and decreases the acoustic emission in the opposite direction.

The acoustic intensity at the same point will be proportional to $(1 - M_c \cos\theta)^{-6}$. In any case, according to (Ref. 11), Lighthill attributes

the factor $(1-M_c \cos\theta)^{-5}$ to the directional distribution of the acoustic intensity.

4.1.1.1.   Discussion of the Factor $(1-M_c \cos\theta)^{-5}$

The directional distribution of the acoustic quadruplet intensity behaves according to $(1-M_c \cos\theta)^{-5}$, and was experimentally verified (Ref. 12, 13) for cold subsonic jets (with respect to the speed of sound in ambiant air), for which the convection Mach number M_c had a value between 0.3 and 0.5.

The case where $M_c > 0.5$ is of great practical importance, since for take-off of transport aircraft, such as the Caravelle, the value of M_c is on the order of 0.9.

For this reason, we will now make several general remarks on this subject.

(1)   The factor $(1-M_c \cos\theta)$ is zero for $\cos\theta = \dfrac{1}{M_c}$. The acoustic radiation will be infinite in this direction, which is physically impossible. The acoustic radiation due to convection of systems of quadruplets cannot concentrate a larger intensity than that of the source itself in this /29 direction.

(2)   According to equation (16), the maximum acoustic pressure is propagated in the direction $\theta=0 (M_c < 1)$

In contrast to this result, the direction θ_M in which the maximum acoustic intensity is received is not the same as the thrust axis (Ref. 6). In addition, the angle θ_M is a function of the velocity of the jet and the diameter (4.1.1.3).

(3)   The acoustic intensity cannot increase indefinitely. It must be assumed that the exponent of the amplification factor which represents the phenomenon of the convection of acoustic sources $(1-M_c \cos\theta)$ must decrease, outside of certain limits, and tend towards zero. The value of M_c, for which the amplification of the acoustic emission due to the phenomenon of convection becomes smaller, remains to be determined.

(4)   We are led to the problem of finding an exponent η for the binomial $(1-M_c \cos\theta)^{-\eta}$ which is no longer constant (for $M_c > 0.5$), but is itself a function of M_c. This value will be determined experimentally.

4.1.1.2. Experimental Research on the Variation of the Exponent η as a Function of M_c

The theory for the convection effect is valid for the entire acoustic spectrum. This is why only the results of the measurements of the total level in decibels are represented as a function of the azimuth θ in Figure 17.

Table VI shows the values of the velocity V_j of the jets and the number M_c. The speed of sound C_a used in the calculation was the one valid for the temperature of 15°.

TABLE VI

VELOCITY V_j AND M_c

Turbojets	Velocity of the Jet V, m/s	Mach No. M_c
Rolls-Royce	250	0,37
Avon RA 29	417	0,61
MK 522	574	0,84
	610	0,90
Karboré II	503	0,74
Atar 9 B 3	608	0,89

In Figure 17, the curves (continuous line) have been calculated in <u>/30</u> each case using the expression $10 \log (1-M_c \cos\theta)^{-2}$. The exponent η was determined by means of successive approximations in order to achieve a satisfactory agreement between the calculated and experimental curves.

It can be seen that for V_j = 250 m/s, the value predicted by theory, η = 5, results in good agreement with experiment for θ > 20°.

For larger jet velocities, smaller values of η must be assumed. Thus, for V_j = 610 m/s, the factor $(1-M_c \cos\theta)$ must only be raised to a power in the vicinity of 2.

Figure 18 shows the variation of η as a function of M_c.

The first conclusion which can be drawn from this experimental study is that for M_c between 0.35 and 0.90, the directional distribution of the total acoustic levels of the jet is proportional to
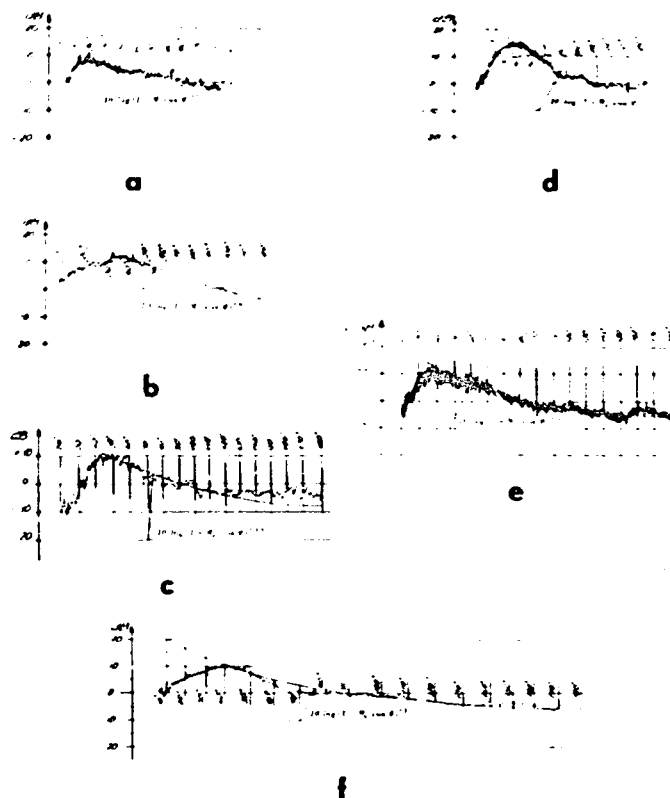
Figure 17

Directional Distribution of Sonic Pressure, in Decibels
with Respect to θ = 90°.

Curve: $10 \log(1 - M_c \cos \theta)^{-}$·

a — AVON RA 29 MK 522, radius 150 m, jet speed 250 m/s.
b — AVON RA 29 MK 522, radius 60 m, jet speed 450 m/s.
c — Marboré II, radius 60 m, jet speed 505 m/s.
d — AVON RA 29 MK 522, radius 150 m, jet speed 574 m/s.
e — ATAR 9 B 3, radius 60 m, jet speed 608 m/s.
f — AVON RA 29 MK 522, radius 60 m, jet speed 610 m/s.

$$(1 - M_c \cos \theta)^{-\eta} \tag{17}$$

The value of η, expressed as a function of M_c, is given by the equation of
the line, shown in Figure 18.

$$\eta = 6 - 3,4 \, M_c \tag{18}$$

33

$$\eta = \mathcal{S} - 3.4\, M_c$$
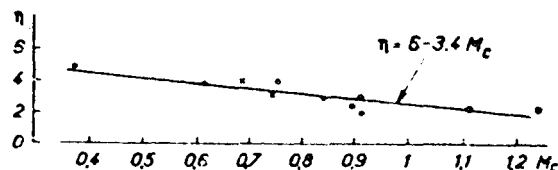
Figure 18

Stationary Jets, Valley of the Exponent η as a
Function of Convection Mach Number M_c

● AVON RA 29 MK 522; × Marboré II; O ATAR 9 K 5 dry
regime; ⊖ ATAR 9 K 5 with afterburner.

4.1.1.3. Experimental Relationship Between θ_M and M_c

A second result obtained from this study is that the
azimuth corresponding to the maximum acoustic radiation, which is the only
significant quantity for our calculations, is also a function of the jet
velocity and of the convective velocity, $M_c C_a$.

The values of θ_M in degrees are shown for five turbojets as a function
of M_c in Figure 19. The effect of the diameter of the jet was neglected.

The equation of the line representing the average variation of θ_M as
a function of M_c is given by

$$\theta_M = 29\, M_c + 16 \tag{19}$$

(θ_M is expressed in degrees).

4.1.1.4. Factor of the Maximum Directional Acoustic Intensity

The directional characteristics of the maximum noise of
stationary jets can be expressed as a function of only the average Mach /31
number of convection of the turbulence in the jet (nevertheless, jets
having a small diameter, such as those of the Marbore II, seem to follow
a slightly different law).

The curve showing the variation of $(M_c \cos\theta_M)^{-\eta}$ (20) as a function
of M_c is shown in Figure 20, where η and θ_M are given by equations (18)
and (19).

$$\theta_M^{\bullet}$$

$$\theta_M^{\bullet} = 29\, M_c + 16$$

Figure 19

Stationary Jets. Angle θ_M of Maximum Sonic Emission
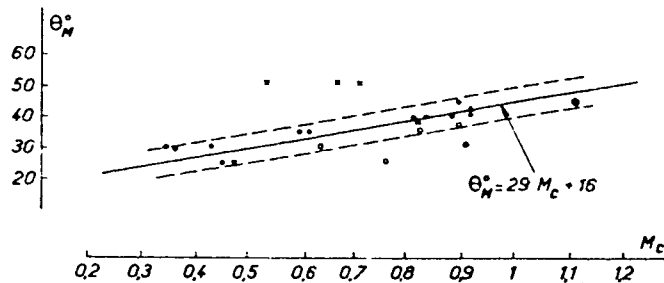as a Function of Convection Mach Number M_c

● AVON RA 29 MK 522; × Marboré II; O ATAR 9 K 5 dry
regime; Δ Verdon; ⊖ ATAR 9 K 5 with afterburner.

The measurement results are also shown in the same figure. The values
shown correspond to the difference between the total acoustic levels along
the direction of the vector corresponding to the maximum acoustic radiation,
and the pressure levels are measured for the azimuth of 90°, the angle for
which the factor $(1-M_c \cos\theta)$ is equal to 1.

It can be seen that the acoustic intensity along the direction of
maximum acoustic radiation increases with the Mach number of convection,
M_c, when the value of M_c remains below approximately 1. The intensity de-
creases after this if the convection velocity becomes larger than 2 C_a.

4.1.2. Calculation of the Maximum Total Acoustic Pressure Levels

After the iso-PNdB-curves have been determined on the ground and
to both sides of the trajectory of an aircraft on take-off, it is possible
to determine, in advance, the distribution of the maximum acoustic pressure
levels along lines parallel to the path of the aircraft.

These acoustic levels are called linear ones, to distinguish them
from polar acoustic levels, which are determined at a constant radial dis-
tance from an aircraft at rest. This latter study was carried out in
3.1.1.2.

After the maximum acoustic levels have been calculated, it becomes
possible to find the laws of variation of polar acoustic levels as a func-
tion of the velocity of the expanded jet. A corrective term is introduced
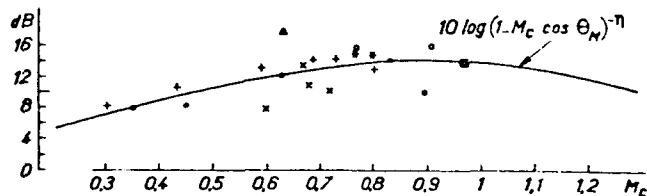
35

Figure 20

Stationary Jets. Sonic Levels Relating to the Angle θ_M°
as a Function of Convection Mach Number M_c

Reference: sonic levels for $\theta = 90°$.

● AVON RA 29 MK 522   X Marboré II   O ATAR 9 K 5
● Verdon   ✳ J 33 A 10 , J 34 WE 34   ▣ AVON RA 29 MK 527
✚ AVON RA 21 R

in order to be able to carry out the transition to the linear acoustic
levels desired. Since the linear acoustic levels are always measured
along the path of aircraft in flight, it becomes possible to compare the
acoustic levels of stationary jets and jets in motion.

4.1.2.1. Maximum Acoustic Pressure in Polar Coordinates

The calculation method consists of determining the
acoustic intensity for the angle at which the convection factor is equal
to 1. The expression obtained is multiplied by the maximum amplification
factor of the acoustic intensity and which is given by (20). It was seen
above (3.1.1.2.) that for $V_j < 2 C_a$, the acoustic power of turbojets, which
operate without an afterburner, is well represented by the Lighthill equa-
tion, equation (1), or by equation (4) in dBp.   /32

The average spatial acoustic level N_m (see 3.1.3.1.) of an acoustic
source which has this power and which radiates uniformly into a hemisphere
having the radius r will be given by the following equation

$$N_m = 10 \log_{10} 5 M_c^3 + C_1 \tag{21}$$

according to (4) and (9), by replacing V_j by $2 M_c C_a$.

The constant C_1 is 132 dB for the adopted radius 30 m (see 3.1.3.3.)
and for the value of the acoustic power coefficient K of $3 \cdot 10^{-5}$, determined
in 3.1.1.2.

36
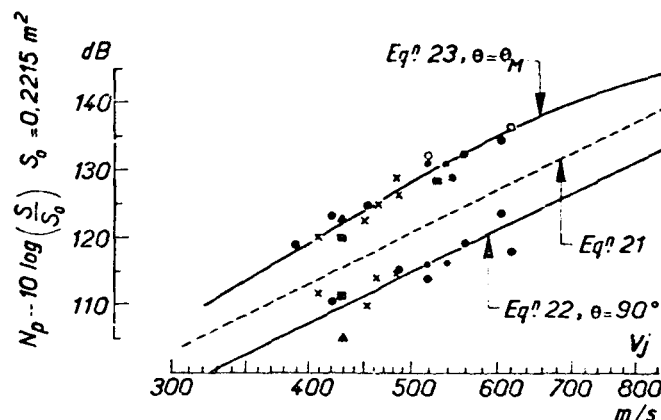
Figure 21

Stationary Jets. Polar Sonic Levels as a Function
of the Jet Speed, Corrected for r = 30 m and S = S_o = 0.2215 m^2

● AVON RA 29 MK 52.   x Marboré II   O ATAR 9 K 5
■ Derwent   ◆ J 33 A 10, J 34 WE 34   ▲ Verdoa   ● Palas

Figure 21 shows the straight line representation of this equation in logarithmic coordinates (dotted line).

The results obtained from equation (21) cannot arbitrarily be retained up to the end of the calculation, because along the direction of θ = 90° the directivity index is not zero (see 3.1.3.2.). This direction is the only one to consider here.

Experiment shows (see also [Ref. 14]) that the value of this index is -6 dB on the average. This causes a change in the constant C_1, such that our acoustic level reference N_r becomes

$$N_r \cdot 10 \log_{10} 5 M_c^? + C_2 \tag{22}$$

with C_2 = C_4 - 6 dB = 132 dB.

Equation (22) is given by the line shown in Figure 21 (a continuous line). This figure also shows the turbojet acoustic levels for θ = 90°, referred to a reference surface of S_0 = 0.2215 m^2 and corrected for r_0 = 30m.
It can be seen that the experimental results confirmed the validity of equation (22) well, which is derived from the dimensional law of Lighthill. Let us recall that this law does not introduce the effect of convection, which is the case under consideration here. For this reason, equation (22)

37

Figure 22

Isobaric Curves, in Decibels, of a Lateral Acoustic
Quadruplet. Diverted Acoustic Field (see text).

(1) Jet axis

no longer needs to satisfy the restrictive condition $M_c < 1$.

Let us now introduce the convection factor in the direction θ_M of
maximum acoustic emission into equation (22), which has already been de-
termined.

The desired maximum acoustic level N_p is thus given by

$$N_p = 10 \, \ell_{g_{10}} \, \frac{S M_c^5}{(1 - M_c \cos \theta_m)^5} + C_2 \tag{23}$$

η and θ_M are given by equations (18) and (19).

The curve calculated according to equations (23) is shown in Figure 21.
The experimental points of Figure 11 which indicate the maximum acoustic <u>/33</u>
levels of the turbojets studied are also shown in this figure.

It can be seen that the experimental results are in satisfactory
agreement with the results of the calculations.

4.1.2.2. Maximum Linear Acoustic Pressure

The relationship between the maximum polar acoustic
levels and the maximum linear acoustic levels can be determined from the
geometrical construction shown in Figure 22. It shows lobes of equal
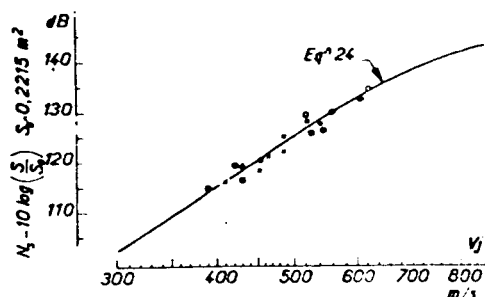acoustic level of a lateral acoustic quadruplet, considered in the far
acoustic field.

38

Figure 23

Stationary Jets. Maximum Linear Sound Levels as a
Function of Jet Speed, Corrected for l = 30 m and
$S = S_0 = 0.2215$ m^2.

● AVON RA 29 MK 522   X Marboré 2   O ATAR 9 K 5
▲ Verdon   ■ Derwent   ◆ J 33 A 10, J 34 WE 34
● Palas

The <u>maximum</u> polar level is given by the point A. This point is de-
fined by the intersection of the polar coordinate vector $r\theta_M$ and the
circle.

Based on the same radius vector, the linear acoustic level at point
B is found, which is the intersection point with the line tangent to the
circle and parallel to one of the symmetry axes of the quadruplet. The
acoustic level at the point B is diminished by $10 \log_{10} \sin^2\theta_M$ with
respect to the acoustic level at A.

The <u>maximum</u> linear acoustic level at point C is given by the <u>tangent</u>
lobe on the right. According to the 1/r law, the acoustic level corres-
ponding to this lobe is larger than 1 dB with respect to the acoustic
level of the lobe which intersects the line at point B.

The relationship between the maximum polar acoustic levels and the
maximum linear acoustic levels has been defined in this way. It can be
seen that the maximum linear acoustic level N_S is given by

$$N_s = 10 \log_{10} \frac{S M_c^5 \sin^2\theta_M}{(1 - M_c \cos\theta_M)^5} + C_3 \qquad (24)$$

where $C_3 = C_2 + 1$ dB = 133 dB for the <u>lateral</u> distance of 30 m.

The linear acoustic levels of turbojets for the measured angles θ_M

39

are shown in Figure 23. They confirm the validity of equations (24).

For an aircraft propelled by n identical jets, the maximum total acoustic level N_T is given by

$$N_T = N_s + 10 \log n \qquad \text{(see 3.1.1.3.)}$$

4.1.3. Generalized Spectrum of the Maximum Linear Acoustic /34 Pressure

The experimental data consist of maximum polar acoustic levels by frequency octaves and by angles θ_M belonging to the frequency intervals. The calculation of the maximum linear acoustic levels was carried out according to the geometrical construction of Figure 22. The calculation was carried out along a line parallel to the jet and tangent to the circle, along which the acoustic levels are known. The total acoustic levels, which are necessary in order to determine the generalized spectrum, were determined by summation of the partial acoustic intensities.

For the lateral distance of 30 m, which was chosen so that the molecular attenuation was negligible, the generalized spectrum of the maximum linear acoustic pressure level is shown in Figure 24.

The coordinates used were:

$$\left. \begin{array}{l} \text{Abscissa, the Strouhal number:} \qquad S_{\ell_{es}} = \dfrac{D}{V_j} f_{es} \\[3mm] \text{Ordinate :} \qquad N_p = \left[N_s - 10 \log \dfrac{V_j}{D} \right] \end{array} \right\} \qquad (25)$$

f_{es} is the frequency emitted by the stationary jets.

In this figure, the continuous curve between the experimental limits shows the average variation of the generalized spectrum. It should be noted that for Strouhal numbers between 0.3 and 0.6, the majority of experimental points is located below this curve. This fact can be attributed to the selective absorption by the Sun, which is encountered in the corresponding frequency interval .

4.2. Jets in Motion

4.2.1. Generalized Spectrum of the Maximum Linear Acoustic Pressure

This generalized spectrum was already obtained (Figure 16). Let us recall that the non-dimensional coordinates used were (see 3.2.2.)
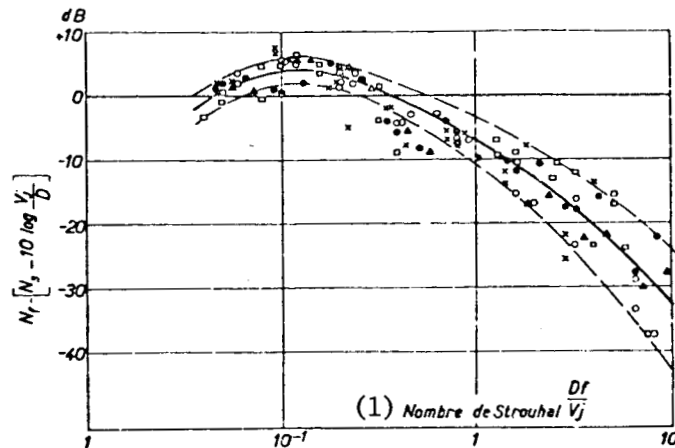
Figure 24

Stationary Jets. General Spectrum of Direction of
Maximum Linear Sonic Pressure, Corrected for 1 = 30 m.

● AVON RA 29 ЧК 522   ◻ Derwent   ○ ATAR 9 K 5
▲ Verdon   × Marboré II

(1) Strouhal number

Abscissa

$$S_{v_e} = \frac{D}{V_j \cdot V_e} f_c$$

Ordinate

$$N_f - \left[N_v \cdot 10 \log \frac{V_j \cdot V_e}{D} \right]$$

(15)

The choice of these dimensionless quantities leads to a representa- /35
tion of the generalized spectrum of jets in motion which is different from
that obtained for stationary jets. This can be seen by comparing Figures
16 and 24.

The representation of these two spectra by means of a __universal__
curve is obviously of interest. This leads to the determination of an
appropriate system of coordinates.

4.2.1.1. Discussion of Dimensionless Quantities (15)

For the velocities V_j and V_e encountered in our experi-
ment, the term $\frac{V_e}{V_j}$ is small with respect to 1. This is also true for the

term $\frac{V_e}{C_a} \cos\theta_M$.

We can therefore set

$$V_j\left(1 - \frac{V_c}{V_j}\right) \approx V_j\left(1 - \frac{V_c}{C_a}\cos\theta_M\right)$$

The Strouhal number of the jet in motion can thus be written as

$$S_a = \frac{D}{V_j(1 - M\cos\theta_M)} f_a \quad \text{where} \quad M = \frac{V_c}{C_a}$$

Let us set $S_{a,0} = S_a$

We have

$$\frac{D}{V_j} f_{es} = \frac{D}{V_j(1 - M\cos\theta_M)} f_a$$

from which

$$f_a = (1 - M\cos\theta_M) f_{es}$$

(26)

Thus, for this relationship, the apparent frequency f_a is lower than the frequency emitted by the stationary jet f_{es}.

The proportionality factor is given by the Doppler effect for $V_c \ll C_a$ for the case where an acoustic source is regressing after having flown over a fixed observer.

In effect, this is the case because, for jet aircraft in flight, the angle θ_M is always acute (Figure 1).

On the other hand, the nondimensional ordinate of the generalized spectrum of jets in motion will be expressed by

$$N_f - \left[N_v - 10\log\frac{V_j(1 - M\cos\theta_M)}{D}\right],$$

The choice of these coordinates does not lead to a coincidence of the generalized spectra of stationary jets and jets in motion. It can be stated that, everything else being equal, the frequencies emitted by the jet in flight are not _identical_ to the frequencies emitted by the stationary jets.

The determination of the relationship between these frequencies leads to another important consequence. It becomes possible to obtain an expression for the acoustic power produced by the jets which is valid _for stationary jets as well as for jets in motion_.
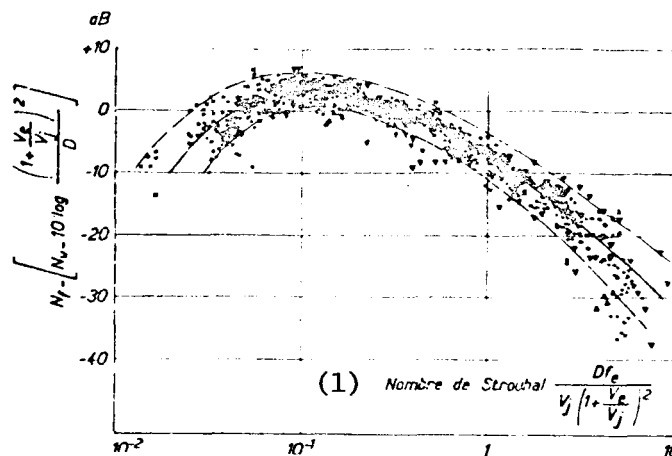
42

Figure 25

Generalized Spectrum of Maximum Sonic Pressure
Corrected for 1 = 30 m.

Aircraft in flight: ● Caravelle; ▮ Gloster Meteor;
O Mirage IV; ▲ Mystère IV A; × Fouga Magister

Stationary aircraft: ▼ (? taken from Figure 24)

(1) Strouhal number

4.2.1.2. Relationship Between the Frequencies Emitted by Stationary Jets and Jets in Motion

In paragraph 2.2 we indicated that the characteristic frequencies, caused by volume sources distributed along the axis of the jet, are proportional to $\frac{V_j}{x}$, where V_j is a characteristic velocity with respect to the tail pipe.

The average velocity of convection of the stationary jet is $\frac{1}{2} V_j$. Thus we have $f_{es} \propto \frac{1}{2} \frac{V_j}{x}$ (27).

For the jet in flight, the average velocity of convection is given by $\frac{1}{2} (V_j + V_e)$ because, with respect to the aircraft, the exterior outflow is parallel to the principal jet and has the same direction as the latter. On the other hand, in the case of the jet in motion, the fixed
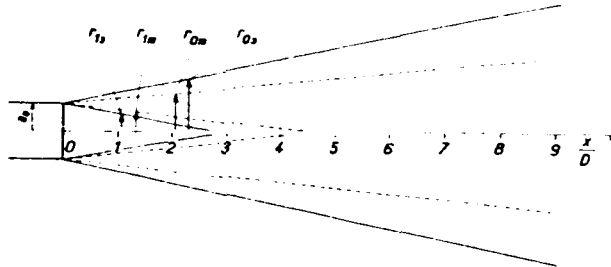
43

Figure 26

Outflow Geometry of Jets (Ref. 16)

—— Atmosphere at rest

- - - $\frac{V_e}{V_j} = 0.25$

observer measures the apparent frequencies f_a. The relationship between these frequencies and the frequency emitted by the jet in flight, f_{ev}, which is given by the Doppler effect, becomes

$$f_a \cdot \frac{1}{1 + M \cos \theta_M} f_{ev}$$

Under these conditions, one finally obtains

$$\frac{f_{ev}}{1 + M \cos \theta_M} \quad \propto \quad \frac{\frac{1}{2}(V_j + V_e)}{x} \tag{28}$$

By combining relationships (27) and (28), on obtains the final result which consists of the ratio between the frequencies _emitted_ by stationary jets and jets in motion, which is written as

$$\frac{f_{ev}}{f_{es}} = (1 + \frac{V_e}{V_j})(1 + M \cos \theta_M)$$

Let us remember that, quite generally, the ratio $\dfrac{V_e}{V_j}$ and the product $M \cos \theta_M$ are small and of the same order with respect to 1. One can form the expression

$$\frac{f_{ev}}{f_{es}} = (1 + \frac{V_e}{V_j})^2 \tag{29}$$

The experimental verification of this relationship is carried out in

44

the following sections.

4.2.1.3. Experimental Results

In (25) let us replace f_{es} by f_{ev}, given by (29).

The nondimensional coordinates of the generalized spectrum of jets in motion will thus be

- Abscissa $\qquad S_{ve} = \frac{D}{V_J (1 + \frac{V_e}{V_J})^2} f_{ev}$

- Ordinate $\qquad N_f - [N_v - 10 \log \frac{V_J (1 + \frac{V_e}{V_J})^2}{D}]$

$$(30)$$

Using these coordinates, Figure 25 shows the results of an analysis of the noise created by five types of aircraft in flight. For comparison purposes, the results obtained for the same aircraft under stationary conditions have been added and were taken from Figure 24. The curve showing the average variation of the generalized spectrum determined for stationary jets is also included.

It can be seen that the generalized spectrum of jets in motion follows the same average curve at the present time. This result therefore confirms the validity of relationship (29). In practice, the noise spectrum of aircraft in flight is expressed in terms of apparent frequencies. This is why nondimensional coordinates are introduced in the calculation of these frequencies, where the Doppler effect is taken into account. These are

- Abscissa $\qquad S_{va} = \frac{D}{V_J + V_e} f_a$

- Ordinate $\qquad N_f - [N_v - 10 \log \frac{V_J + V_e}{D}]$

$$(31)$$

4.2.2. Acoustic power of jets in Motion

The acoustic power of jets in motion can be determined by dimensional analysis, based on the results obtained previously for stationary jets.

In 3.1.1.1., from (Ref. 3), we found the relationship

$$w_s \sim f_a \, S \, V_J^4 \, f_{es}^2 \, L_s^4 / c_a^5 \qquad (32)$$

w_s is the acoustic power of the subsonic stationary jet and f_{es} and L_s are a characteristic frequency and a characteristic dimension of the turbulence, respectively.
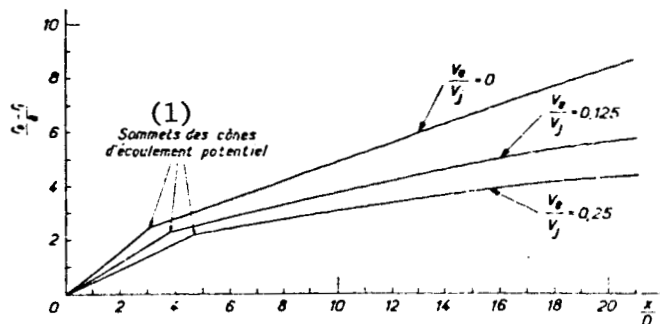
Figure 27

Effect of Secondary Outflow (Ref. 16)

(1) Peaks of potential outflow cones

For the jet in motion, the velocity which enters into the calculation of the acoustic power w_{av}, is $(V_j - V_e)$. Therefore, one

$$w_v \sim \rho_e \, 5 \, V_j^4 \left(1 - \frac{V_e}{V_j}\right)^4 f_{ev}^4 \, L_v^2 / c_e^5 \qquad (33)$$

f_{ev} is a characteristic frequency of the jet in flight this time. L_v is /38 a characteristic dimension of the turbulence of this jet.

The relationship between the acoustic power of jets in flight and stationary jets is thus defined, under the condition that a relationship between L_s and L_v is established. It is assumed that the ratio of f_{es} and f_{ev} is given by (29). Kraichnann (Ref. 15) showed theoretically that there is a relationship between the turbulence scale and the associated acoustic wave, such that for a given turbulence wave number there is a corresponding acoustic wave for the same wave number. It follows from equation (29) that the development of the turbulence of stationary jets and jets in motion will not be the same along the axis of the jet.

This hypothesis was corroborated by the calculations of Squire and Trouncer (Ref. 16), who studied the structure of coaxial jets. These authors determined the equations of motion of a round jet in an incompressible fluid, subjected to external outflow in the same direction as that of the jet. They showed that the cone of outflow potential is extended and the angle of expansion of the jet is diminished for a jet in an atmosphere at rest. The numerical solutions (Ref. 16) of their equations (Figure 26) show the radius of the jet r_0 and the radius of the cone of outflow potential r_1 referred to the radius of the nozzle a, for
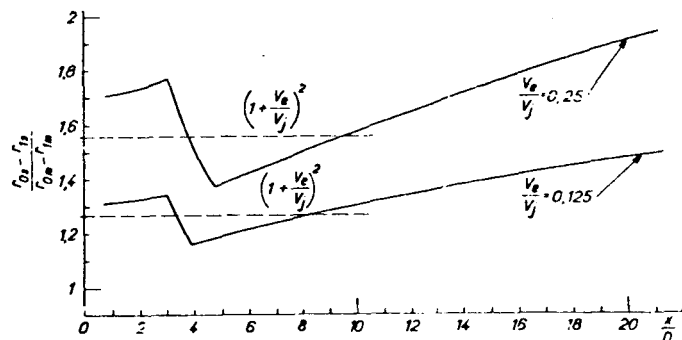
Figure 28

Relative Variation of Zones of Turbulence of Jets

discrete values of $\frac{V_e}{V_j}$, as a function of $\frac{c^2 x}{a}$. c^2 is a length coefficient of the mixing zone, equal to 0.0067.

Figure 27 shows the variations of the term $\frac{r_{0s} - r_{1s}}{a}$, for a jet operating in an atmosphere at rest, and of $\frac{r_{cm} - r_{1m}}{a}$ of the jet subjected to the coaxial outflow V_ℓ, as a function of $\frac{x}{D}$, which is the number of diameters.

Figure 28 shows the variation of the ratio $\frac{r_{0s} - r_{1s}}{r_{0m} - r_{1m}}$, as a function of $\frac{x}{D}$, for $\frac{V_e}{V_j}$ of 0.125 and 0.25. This corresponds to our experiments on jets in flight.

Before interpreting the curves, let us recall that the acoustic power emitted by a unit length of the jet remains constant in the mixing zone (x_0 law). It then decreases abruptly according to the x^{-7} law (Ref. 4), downstream from the apex of the outflow cone, that is, for $\frac{x}{D}$ larger than 8.

It follows that for $\frac{x}{D} > 15$, the acoustic power emitted by a unit length becomes negligible for practical purposes.

If we consider Figure 27 again, it can be seen that for $\frac{x}{D} \leq 15$ each of these curves can be represented by a line parallel to the abscissa axis

47

and which has the ordinate value $(1 + \frac{V_e}{V_j})^2$, if we are willing to tolerate a maximum error of $\pm 10\%$. This approximation causes an error of ± 0.5 dB in decibels units, which is completely acceptable.

Figure 28 shows these lines (continuous lines). Since the differences $r_{0s} - r_{1s}$ and $r_{0m} - r_{1m}$ also corresponds to the characteristic lengths of the vortices L_s and L_v, we may also write

$$\frac{L_s}{L_v} = (1 + \frac{V_e}{V_j})^2 \qquad (34)$$

By combining equations (29) and (34), one finally obtains

$$f_{ev} L_v = f_{es} L_s \qquad (35)$$

Thus, the product of a characteristic frequency and a characteristic dimension of the vortex is a characteristic velocity. It can thus be seen that this product does not depend on the velocity with which the jet is transported V_e.

From (35), expression (33) can also be written as

$$w_v \sim \ell_a S V_j^4 (1 - \frac{V_e}{V_j})^4 f_{es}^4 L_s^4 / c_a^5 \qquad (36)$$

By replacing $f_{es}^4 L_s^4$ by V_j^4, and by introducing the coefficient of acoustic power K, we finally obtain

$$w_v = K \ell_a S V_j^8 (1 - \frac{V_e}{V_j})^4 / c_a^5 \qquad \text{with } K = 3 \cdot 10^{-5} \qquad (37)$$

It can be seen that for $V_e = 0$, the expression for the acoustic power of the jet in flight, which has been established by a dimensional analysis, is reduced to Lighthill's equation (Ref. 3), which is valid for stationary jets.

4.2.3. Directional Distribution of the Acoustic Intensity

For a jet transported at the velocity V_e from the aircraft, the Mach number of convection must be referred to the atmosphere and can be written as $\frac{1}{2}(\frac{V_j - V_e}{c_a})$, where, in our notation, $(M_c - \frac{M}{2})$, $M = \frac{V_e}{c_a}$ is the Mach number of the aircraft.

According to the theory of Lighthill (Ref. 3), the directional

intensity of the noise of subsonic jets contains the factor

$$[1-(M_c - \frac{M}{2})\cos\theta]^{-\tau} \tag{38}$$

Ffowes Williams (Ref. 17) calculated that conduction effects introduce an overall factor given by

$$[1-(M_c - \frac{M}{2})\cos\theta]^{-\tau}(1+M\cos\psi)^{-1} \hspace{2cm} \underline{/40}$$

ψ is the angle of acoustic emission referred to the axis of the jet in flight.

The acoustic intensity received on the ground by a fixed observer depends, among other things, on the Doppler effect, such that the expression given by Lighthill becomes

$$[1-(M_c - \frac{M}{2})\cos\theta]^{-\tau}(1+M\cos\theta)^{-1} \tag{38}$$

A comparison of the terms (20) and (38) shows that the directional characteristics of the noise of stationary jets is different from those of jets in motion.

Thus, the same will hold for the directivity indices.

4.2.3.1. Factor of Maximum Directional Acoustic Intensity

The definition of the directional factor of maximum acoustic intensity becomes easier by analytically studying the stationary jet.

If we include the case where the convection Mach number is larger than 0.5, we will stipulate for jets in motion that the maximum convection factor is of the form

$$[1-(M_c - \frac{M}{2})\cos\theta_M]^{-\tau}$$

θ_M and η are given by equations (19) and (18).

We have thus assumed, for the meantime, that the emission angle of maximum acoustic radiation follows the law determined for stationary jets.

The amplification predicted by this factor is, in any case, reduced due to the Doppler effect, expressed as $(1 + M \cos\theta_M)^{-1}$. The maximum
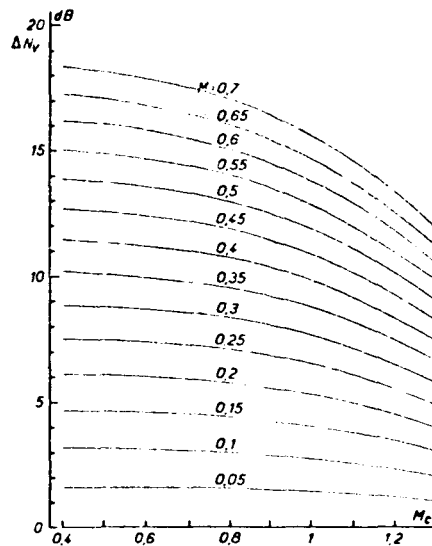
Figure 29

Monogram which Shows the Reduction ΔN_V of Maximum Sonic
Levels for Discrete Values of Flight Mach Numbers

acoustic intensity received on the ground finally contains the following
product as a factor

$$[1-(M-\tfrac{M}{2})\cos\theta_m]^{-7}\ (1+M\cos\theta_m)^{-4} \tag{39}$$

4.2.4. Reduction of the Maximum Directional Acoustic Intensity on the Ground Produced by the Transport Velocity of the Jets /41

This reduction of the acoustic intensity can be determined, on
the one hand, by the relationship between the factors (20) and (39), and,
on the other hand, by the reduction of the acoustic intensity which belongs
to the source itself.

A comparison of equations (2) and (37), which express the acoustic
power of stationary jets and jets in flight, shows that the motion of the
jet causes a reduction of the acoustic power which is proportional to
the factor $(1 - \frac{V_e}{V_j})^4$. This will also be the case for the average acoustic
intensity, transmitted by a surface unit element normal to the direction
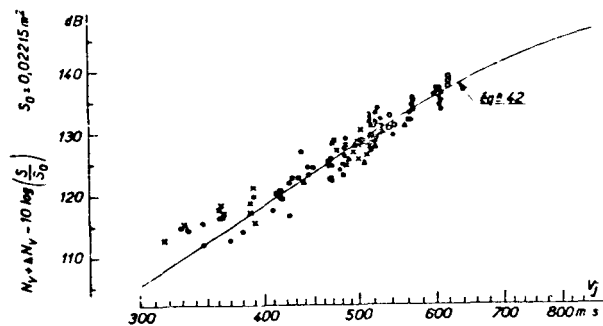of propagation of the acoustic waves.

50

Figure 30

Aircraft in Flight. Maximum Sonic Levels Corrected by
Equation (40) as a Function of Jet Speed

$S = S_o = 0.2215$ m and $1 = 30$ m

● Caravelle   ■ Gloster Meteor   O Mirage IV
▲ Mystère IV A   × Fouga Magister

Let us recall the ratio $\dfrac{V_e}{V_j}$ encountered in our experiments. The binomial $(1 - \dfrac{V_e}{V_j})^4$ can be expressed by $(1 + \dfrac{V_e}{C_a} \cos\theta_M)^{-4}$, which introduces the angle of maximum acoustic emission.

From the above, the reduction of the acoustic levels ΔN_v is given by

$$\Delta N_v = 10 \log_{10} \frac{[1-(M-\frac{M}{2})\cos\theta_m]^3 (1+M\cos\theta_m)^6}{(1-M_c\cos\theta_m)^7} \tag{40}$$

Figure 29 shows the grid of these curves, calculated by means of this equation, for discrete values of M between 0.1 and 0.7.

Equation (40) assumes that the angle θ_M of maximum acoustic radiation is not affected by the motion of the jet and assumes, in an implicit way, that the index of directivity which enters in the expression of the reference acoustic level of the stationary jet (4.1.2.1.) is the same as for the jet in motion. The correction δN_v required due to these approximations can be determined experimentally by setting

$$\delta N_v = (N_v + \Delta N_v) - N_s \tag{41}$$

51

N_V is the acoustic level measured along the path of the aircraft
and

N_S is given by equation (24).

Let us recall that equation (24) expresses the acoustic levels distributed along a line parallel to the axis of the jet. In our experiments, the acoustic levels of aircraft in flight were recorded during overflights at constant altitudes and also during take-off. The angle of ascent did not exceed 10°.

In the latter case, the correction to be applied to (24) is negligible. For an angle α which the jet makes with the horizontal axis of $\alpha_0 = 0°$ to $\alpha_1 = 10°$, the maximum acoustic levels measured during the /42 ascent of the aircraft varied according to $10 \log \dfrac{\cos^2\alpha_0}{\cos^2\alpha_1}$. This amounts to barely 0.1 dB.

The acoustic levels N_V of aircraft in flight, determined by the conditions specified in 3.2.1., were corrected by means of equation (40) and are shown in Figure 30 as a function of V_j alone. Under these conditions, it can be seen that the curve showing the average variation of the acoustic levels of various types of aircraft follows the law determined for stationary jets (24) to a satisfactory approximation, under the condition that this curve is translated by + 3 dB.

The experimental value of δN_V having been determined and introduced in (41), we find that

$$N_V - N_S = \Delta N_V + 3 \, dB \tag{42}$$

ΔN_V is given by (40).

4.2.5. Maximum Total Acoustic Pressure

The equation of the maximum total acoustic pressure levels received on the ground and produced by subsonic aircraft in flight can be determined by writing equation (42) explicitly.

This equation is

$$N_V = 10 \log \frac{S \, M_c^5 \, \sin^2\theta_M}{[1 - (M_c - \frac{M}{2}) \cos\theta_M]^\eta (1 + M\cos\theta_M)^5} + C_4 \tag{43}$$

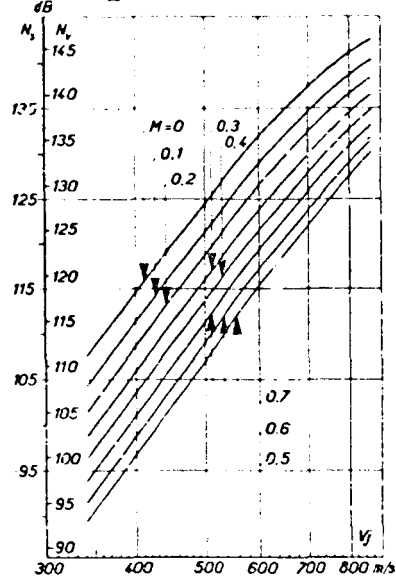η and θ_M are given by (18) and (19).

Figure 31

Monogram Showing Maximum Total Sonic Levels for Jet
Aircraft on the Ground and in Flight for the Lateral
Distance or Geometric Altitude of 30 m.

Corrections:

For $S \neq S_o$, add $10 \log \dfrac{S}{S_o}$.

For n turbojets on the ground, add $5 \log n$.

For n turbojets in flight, add $10 \log n$.

(1) Ground; (2) Flight

For ℓ = 30 m, where ℓ is the distance to the aircraft, the constant C_4 is equal to C_3 + 3 dB, i.e., 136 dB.

It can be seen that for M = 0, equation (43) is reduced to (24) with a difference of about 3 dB.

The numerical solutions of equation (43) are shown by the curve, in Figure 31. These curves were calculated for values of M_c for 0.5 and 1.2. M was varied from 0 to 0.8, in steps of 0.1.

53

5. Conclusions

The analytical study of jet noise of stationary aircraft and sub-sonic aircraft in flight shows that it is possible to determine the maximum acoustic pressure received on the ground. This can be done beforehand and in a satisfactory way.

The method of calculation is based on the law of Lighthill for the /43 variation of the acoustic power with $SV_j{}^8$. The following effects must be added: The amplification of the acoustic intensity due to the convection factor (stationary jet and jet in motion), the noise reduction factor given by an aerodynamic effect, and the attenuation factor given by the Doppler effect.

The result of these calculations has been verified for turbojets without afterburners and without jet silencers. It is valid for convection Mach numbers up to 1.2 and flight Mach numbers up to 0.7.

The acoustic pressure levels by frequency bands are determined by a generalized spectrum of the maximum acoustic pressure. These are plotted as a function of coordinates so that they are the same for stationary jets and jets in motion.

An important result is the isolation of an aerodynamic effect on the turbulence of the jet, which is a function of $(1 + \frac{V_e}{V_j})^2$ which causes a shift of the emitted frequencies and a division of the acoustic intensity by the factor $(1 + M \cos\theta_M)^4$.

REFERENCES   /44

1. Coles, G. M. Estimating the Jet Noise. The Aeronautical Quarterly, Feb., 1963.
2. Laurence, J. C. Intensity, Scale and Spectra of Turbulence in Mixing Region of Free Subsonic Jets. N.A.C.A. Rep., 1292, 1956.
3. Lighthill, M. J. On Sound Generated Aerodynamically - Part I., General Theory. Proc. Roy. Soc., Vol. A, 211, 1952; and Part II, Turbulence as a Source of Sound. Proc. Roy. Soc., Vol. A, 222, 1954.
4. Lighthill, M. J. Sound Generated Aerodynamically. Proc. Roy. Soc., Vol. A, 267, 1962.
5. Cole, J. N. and associates. Noise Radiation from Fourteen Types of Rockets in the 1000 to 130,000 Pounds Thrust Range. Wright Air Devel. Center, Rep. 57, 354.
6. Powell, A. On the Generation of Noise by Turbulent Jets. Aviation Conf., Los Angeles, Calif., March, 1959 (Publ. A.S.M.E.).
7. Kobrynski, M. On the Structure of the Acoustic Field of Turbojets,

2nd International Congress of Acoustics, Cambridge, U.S.A., June, 1956. La Rech. Aéron., No. 58, May-June, 1957.

8. Wiener, F. M. Sound Propagation Outdoors. Noise Control, July, 1958.

9. Greatex, F. B. Take Off and Landing of the Supersonic Transport. Aircraft Engineering, No. 8, Vol. XXXV, August, 1963.

10. Kobrynski, M. Contribution to the Study of Rocket Noise. 4th International Congress of Acoustics, Copenhagen, Denmark, August, 1962. Note Technique, O.N.E.R.A., No. 74, 1964.

11. Ffowes Williams, J. E. On Convected Turbulence and Its Relation to Near Field Pressure. Univ. Southampton Aero. Ast., Rep. 109, 1960.

12. Lee, R. Free Field Measurements of Sound Radiated by Subsonic Jets. Taylor Model Bassin, Washington D.C.,Rep. 868, 1953.

13. Lassiter, L. W., Hubbard, H. H. Experimental Studies of Noise from /45 Subsonic Jets in Still Air. N.A.C.A. Techn. Note, No. 2757, 1952.

14. von Gierke, H. E. Aircraft Noise Sources. Handbook of Noise Control, McGraw-Hill Co., N. Y., 1957.

15. Kraichnann, R. H. The Scattering of Sound in a Turbulent Medium. J.A.S.A., 25, 1953.

16. Squire, H. B., Trouncer, J. Sound Jets in a General Stream. ARC Rep. and Memo, 1904, 1944.

17. Ffowes Williams, J. E. The Noise from Turbulence Convected at High Speed. Phil. Trans. Roy. Soc., Series A, 255, 1963.

18. Kryter, K. D. The Meaning and Measurements of Perceived Noise Level. Noise Control, Vol. 6, No. 5, Sept.-Oct., 1960.

19. Kryter, K. D., Pearsons, K. Some Effects of Spectral Content and Duration on Perceived Noise Level. J.A.S.A., Vol. 35, No. 6, June, 1963.

20. Kobrynski, M. On the Generalization of the Calculation of the Noise of Jet Aircraft. 5th International Congress of Acoustics, Liege, Belgium, September, Comm. I, 45, 1965.

CALCULATION OF THE MAXIMUM ACOUSTIC PRESSURE

Input Quantities

n – Number of turbojets, which all have the same motor parameters.

s – Output surface of a pipe

M_c – Convection Mach number $= \frac{1}{2} \frac{V_i}{C_a}$.

M – Rolling Mach number and flight Mach number, $M = \frac{V_a}{C_a}$.

Desired Quantities

The number of P.N.dB on the ground, at a distance L of the aircraft for three configurations of the aircraft:

- Instant when the brakes are released.

- During rolling.

- During ascent.

The stages in the calculation are the same in all the cases:

(1) – Calculation of the total linear acoustic pressure level N_T, corresponding to the interval 20-10,000 cycles for a reference distance of $\ell = 30$ m.

(2) – Calculation of the distribution of the acoustic levels by frequency octaves, for the same reference distance.

(3) – Calculation of the acoustic levels by frequency octaves for the distance L >> 30 m.

(4) – Conversion to P.N.dB.

1. TOTAL ACOUSTIC LEVEL FOR $\ell = 30$ m   /47

Instant of Releasing the Brake

The acoustic level N_T is given by the equation

$$N_T = 10 \log_{10} \frac{S M_c^{\ell} \sin^2 \theta_n n^{\frac{1}{2}}}{(1 - M_c \cos \theta_n)^{\eta}} + 133 \; dB$$

where $\eta = 6 - 3.4 \, M_c$

and $\theta = 29 \, M_c + 16$.

56

This calculation was considerably simplified by use of the chart shown in Figure 31. For M = 0, the value of N_S corresponding to the jet velocity V_j is read off. N_T is then given by

$$N_T = N_s + 10 \log_{10} \frac{S_n \, i}{S_o} \quad dB \tag{1}$$

Rolling

The acoustic level N_T is determined by

$$N_T = 10 \log_{10} \frac{S \, M_c^8 \, \sin \theta_n \, x \, \frac{i}{i}}{[1-(M_c - \frac{M}{2}) \cos \theta_n]^4 (1 + M \cos \theta_n)^5} + 135 \, dB$$

Using the chart (Figure 31), the value of N_S corresponding to V_j is read off, for M given. N_T is then found from equation (1).

Ascent

The acoustic level N_T is calculated from

$$N_T = 10 \log_{10} \frac{S \, M_c \, \sin^2 \theta_n}{[1-(M_c - \frac{M}{2}) \cos \theta_n]^4 (1 + M \cos \theta_n)^5} + 136 \, dB$$

Using the chart, the value of N_V corresponding to V_j is determined, for M given. N_T is then obtained from

$$N_T = N_V + 10 \log_{10} \frac{S_n}{S_o} \quad dB$$

2. ACOUSTIC LEVELS BY FREQUENCY OCTAVES

2.1. Distance Equal to 30 m

For the three aircraft configurations, the acoustic level for the octave i, N_{Ti}, is calculated using the mean curve of the generalized spectrum of jets in flight, which is called the fundamental curve (Figure 32, average curve of Figure 25).

The coordinates that must be used are

as the abscissa $\quad \frac{D}{V_j + V_e} f$

as ordinates $\quad N_i \, [N_V - 10 \log_{10} \frac{V_j + V_e}{D}]$
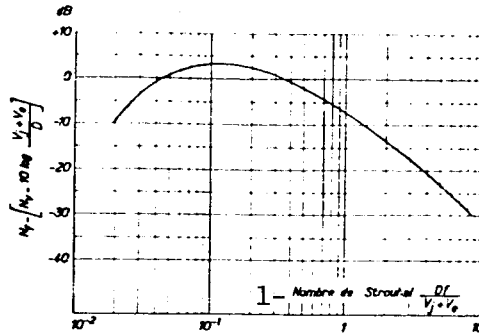
57

Figure 32

Stationary Aircraft and Aircraft in Flight. Curve Showing
the Average Variation of the Generalized Spectrum of
the Maximum Sonic Pressure as a Function of
Strouhal Number.

(1) Strouhal Number.

The desired value of N_{Ti} is determined by

$$N_{T_i} = N_T + 10 \log_{10} \Delta f_c - 10 \log_{10} \frac{V_j + V_e}{D} + K_i \tag{2}$$

Δf_c is the frequency integral of the octave 1.

K_i is positive or negative, and is the number of decibels read
along the ordinate of the curve for the abscissa
$\frac{D}{V_c + V_e} f_c$.

f_c is the central frequency corresponding to the octave 1.

Let us note that for the aircraft at rest, $V_e = 0$ and n_i is
determined for the abscissa $\frac{D}{V_j} f_c$.

2.2. Distances Larger than 30 m

For a distance L larger than 30 m, the acoustic level of the octave i,
N_{Ti}, is determined by the equation

$$N_{i} = N_{T_i} - 20 \log \frac{L}{l} + 20 \alpha (L - l) \log e$$

58

$\ell = 30$ m and α is an attenuation coefficient which is dependent on /49 the atmosphere characteristics and the frequency.

The chart shown in Figure 13 makes it unnecessary to carry out calculations of the geometric and molecular attenuations. This grid of curves was calculated (Ref. 8) for the atmosphere at rest, which has the following characteristics: standard pressure, temperature 15° and hygroscopic state of 50%. Let us note that the I.S.O. has recommended that the value 70% be adapted for the hygroscopic state.

3. CALCULATION OF THE NORMALIZED PERCEPTIBLE AUDIBLE LEVELS (pndb)

The transformation into P.N.dB. of the acoustic levels given in terms of frequency band and determined from the generalized spectrum of maximum acoustic pressure levels, is carried out by the method of Stevens, which was modified by Kryter (Ref. 18).

The normalized audible perception level is given by

$$P.N\,dB = \frac{1.2 + \log_{10} S_T}{0.03}$$

S_T is the sonority in "noys" of the total noise

$$S_T = S_M + F\,(\Sigma S \cdot S_M)$$

S_M is the number of "noys" of the most sonorous octave

ΣS is the total number of "noys" of all the frequency bands of the interval 20-10,000 cycles.

F is a factor which equals 0.3 in the case where the analysis is carried out by frequency octaves.

The number ΣS is given by the sum of "noys" determined for each frequency octave according to an experimental table (Ref. 18).

Recently, Kryter and Pearsons (Ref. 19) published a new conversion table which results in values of pndb which are slightly different.

Scientific Translation Service
4849 Tocaloma Lane
La Canada, California